UKIRT NEWSLETTER

UNITED KINGDOM INFRARED TELESCOPE

SPRING 2009 · #24

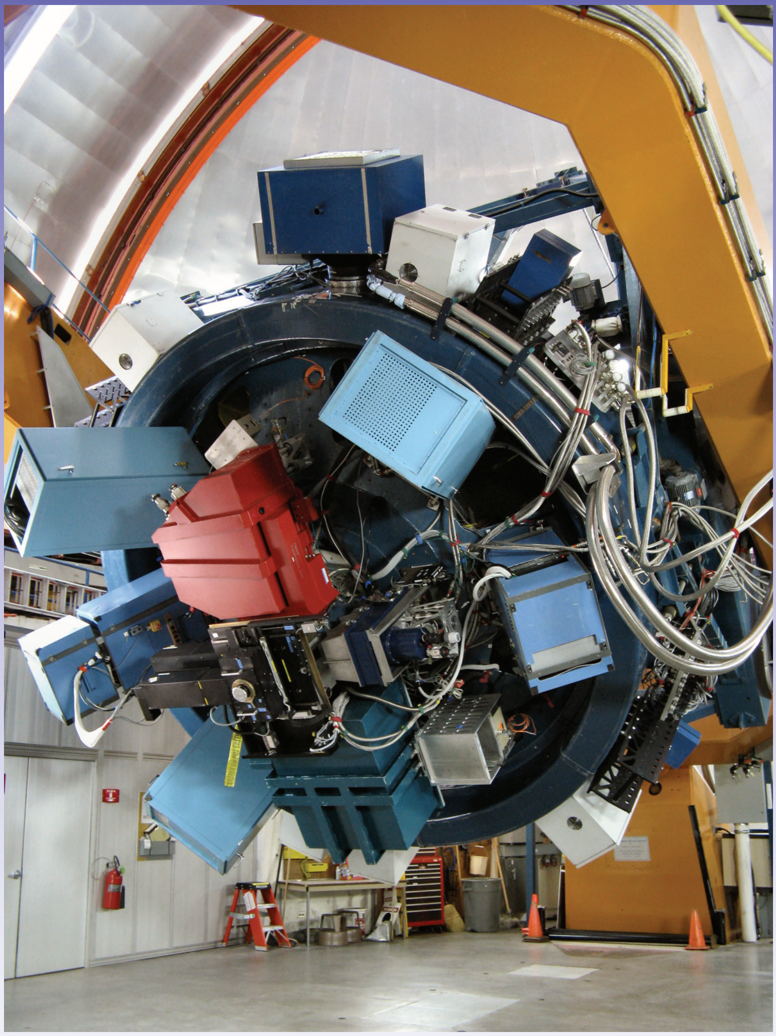

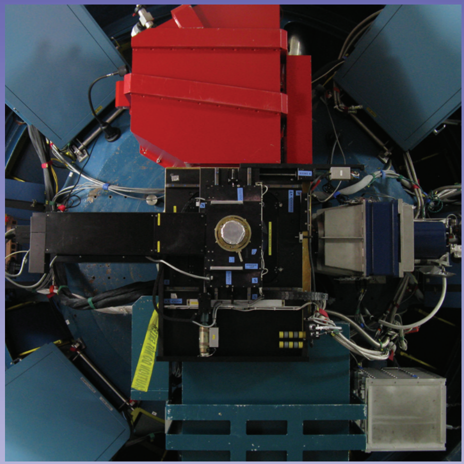

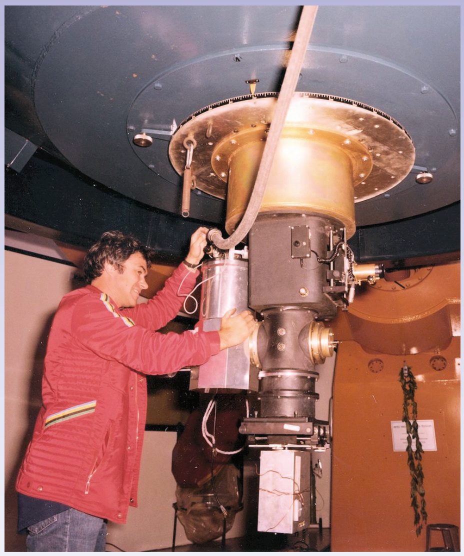

Then and Now

30 years of UKIRT Cassegrain instrumentation

Cassegrain Science Results

Cassegrain Reflections

In This Issue

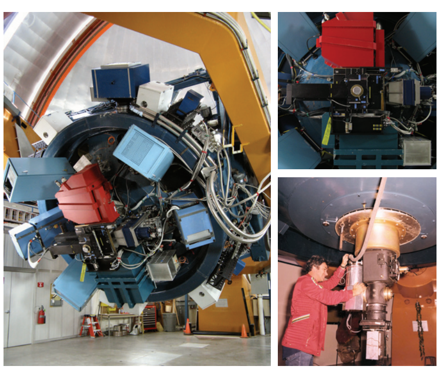

On the front cover: Up periscope! Photos showing the development of Cassegrain instrumentation at UKIRT, from shortly after the commissioning in 1979 (lower right), to the present day (left and upper right). The handsome-looking chap leaning against one of the first "UKT" instruments in the earlier photo is Terry Lee: the four Cassegrain ports in the recent photo are occupied by CGS4 (red, top — north port), UFTI (royal blue, right — west port), UIST (turquoise, bottom — south port) and the wavefront sensor (black, left — east port). (Also see Figure 1 and article on page 20; images courtesy Jonathan Kemp/JAC and Royal Observatory Edinburgh.)

On the rear cover: Celebrating the International Year of Astronomy, Hawaiian style. Featured JAC staff include Inge Heyer (upper left), Andy Adamson (upper right), Luca Rizzi (lower right), and Frossie Economou (lower left). Also, Journey through the Universe astronomers (center). (Also see article on page 4; images courtesy Inge Heyer/JAC.)

UKIRT Newsletter, United Kingdom Infrared Telescope, is published bi-annually and is edited by Chris Davis and Jonathan Kemp.

ISSN 0143-0599.

postal address
United Kingdom Infrared Telescope
Joint Astronomy Centre
University Park
660 North A'ohoku Place
Hilo, Hawai'i 96720-2700
USA

telephone
+1 (808) 961 - 3756

facsimile
+1 (808) 961 - 6516

world wide web
http://www.jach.hawaii.edu/UKIRT/

The Joint Astronomy Centre provides services and support to enable visiting and staff astronomers to undertake top-quality, front-line international-class research using the James Clerk Maxwell Telescope (JCMT) and the United Kingdom Infrared Telescope (UKIRT); to develop these facilities in order to maintain their position as the most advanced of their kind in the world; to operate them in the most cost effective and efficient manner on behalf of the funding agencies; and to be responsive to the changing needs of the contributing organizations.

UKIRT is supported by the United Kingdom's Science and Technology Facilities Council (STFC); it is overseen by the UKIRT Board.

UKIRT is a member of the Opticon trans-national access programme.

Science & Technology Facilities Council

Top End

Professor Gary Davis (*Director JAC*) & Andy Adamson (*Associate Director UKIRT*)

Gary Davis, Director JAC

Welcome to the Spring 2009 issue of the *UKIRT Newsletter*. The telescope has undergone a profound change since our last column, and although this has reduced UKIRT's range of scientific capabilities, we are currently in the midst of developing a proposal for an exciting future.

We wrote in the previous issue that, following STFC's Programmatic Review, UKIRT's future operating mode would be selected in December 2008 from a menu of possibilities. As most readers are probably aware by now, the selected option was to operate exclusively in wide-field mode, with WFCAM as the only instrument, with the scientific objective of completing the UKIDSS programme as expeditiously as possible. We estimate the completion of UKIDSS in mid-2012 and it is gratifying that, despite the severe financial pressures on the organisation, STFC were prepared to make this commitment to UKIRT's top-priority science programme.

An unfortunate consequence of moving to wide-field mode is that the three Cassegrain instruments, CGS4, UFTI and UIST, were removed from service following the last scheduled Cass night on 25th January. This is a profound change of operating mode for the observatory and its staff, and I can confirm that the Board took this decision only after much deliberation and with great regret. To mark the occasion, this issue of the *Newsletter* is devoted to science results from these instruments. It is conceivable that the Cass instruments will be returned to service at some point, depending on the outcomes of two reviews (one in the UK and one in Europe) and of discussions with potential partners.

Although the observatory's priority is now to complete the approved UKIDSS survey as quickly as possible, we are working closely with the Board to ensure that the scientific programme is optimised within that constraint. An analysis of the telescope time and of the observatory's support capacity indicates that we can continue to offer limited amounts of Campaign, PATT and Service time without compromising the UKIDSS end date. Accordingly, a Call for Proposals for semester 09B was issued in February and it is rewarding to note that the oversubscription is back to its normal value of around 2.

The cessation of Cassegrain operations brings to an end one of the less recognized aspects of UKIRT operations over the past few years: the opportunity for visiting observers to undertake (willingly or otherwise!) observations with instruments and in science fields with which they were not familiar. The final visiting observers of the Cassegrain block observed X-ray absorbed QSOs with UIST, but while at the telescope successfully used all three Cass instruments on projects as diverse as studies of H_3^+ in the ISM (CGS4 echelle), the atmospheres of pulsating Carbon stars (UIST spectroscopy), and even followed up a γ-ray burst with UFTI!

December saw the completion of the CGS4 upgrade project, and it is good to be able to report that the upgraded instrument performed extremely well. It is a pity that the opportunity to benefit was not more extended but, should Cassegrain operations return in the future, CGS4 will be there with an all-new ARC array controller and PC-based acquisition system.

As noted above, the completion of UKIDSS will take us up to mid-2012. The future of the observatory beyond that date is contingent on the outcome of a proposal now in preparation. Prof. Hugh Jones (Hertfordshire) submitted a Statement of Interest to STFC in February for a new instrument called UKIRT Planet Finder (UPF). The primary science goal of this instrument is to search for Earth-mass planets in the habitable zones around their parent stars by extending the radial velocity technique into the infrared and surveying nearby M dwarfs. This is one of the highest priorities in all of astrophysics and, if this project is ultimately approved, it will keep UKIRT at the forefront of astronomy for several years to come. The instrument itself is a high-stability, high-resolution spectrograph operating over the *YJH* bands, and will therefore be applicable for many other areas of science as well. The Statement of Interest was endorsed by PPAN and a full proposal has been invited; it is currently being prepared and will be submitted to PPRP in early May. The approval process is likely to run until the end of the year. We are grateful to Hugh and to the UKATC for taking this forward.

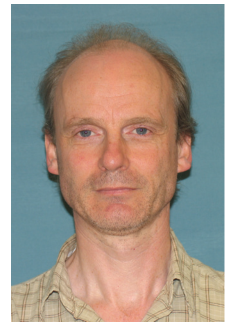

Andy Adamson, Associate Director UKIRT

Finally, UKIRT will celebrate its 30th anniversary later this year. To mark this occasion, we are organising a science workshop at the UKATC in mid-September to celebrate three decades of science with UKIRT and to look forward to the future. Details of this will be announced shortly and we warmly invite all UKIRT users to attend and participate.

An Update from the WFCAM Science Archive (WSA)

Mike Read (*Edinburgh*)

Hosted by the Wide-Field Astronomy Unit (WFAU), Edinburgh, the WFCAM Science Archive (WSA) holds processed WFCAM data for both the UKIRT Infrared Deep Sky Surveys (UKIDSS) and private, non-survey, programmes.

The most recent database release of proprietary UKIDSS data, DR4, contained some 1.6 Tb of ingested catalogue data. Pixel and catalogue FITS files held on disk now amount to over 65 Tb.

Access to the data is via WFAU's website (http://surveys.roe.ac.uk/wsa/). Users must be registered to access proprietary UKIDSS and non-survey data, although data for which the proprietary period has passed are available through WORLDOPENTIME and WORLDR2 database releases. WFAU also publishes the UKIDSS databases to the Virtual Observatory via the Astrogrid infrastructure.

Following on from initial flat-file access, registered non-survey projects (from the PATT, UKIRT service, University of Hawaii, Korean and Japanese queues) will be published to their own released databases. Recently a largely automatic scheme has been implemented to speed up and enhance this database product. Depending on the type of observations made, the enhancements include variability/synoptic tables and the generation of deep image stacks. For more details see http://surveys.roe.ac.uk/wsa/nonSurveyDB.html and the linked ADASS papers. Non-survey PIs are also encouraged to check the status of their projects via the nonSurvey link on the WSA sidebar.

Please also remember that non-survey projects must be registered with WFAU. This does not happen automatically! See the "Accessing Flexed Data" link on the UKIRT homepage sidebar, the nonSurvey page at WFAU, or the WFCAM "Reduction cookbook", which is also available via the UKIRT homepage sidebar.

The WFCAM Science Archive website now provides a facility for generating colour images of up to 1'×1' in size. Some example images from UKIDSS data are presented with this article.

Questions about the archive should be addressed to wsa-support .at. roe.ac.uk .

Celebrating the International Year of Astronomy, Hawaiian Style

Inge Heyer (*JAC Outreach Specialist*)

As many readers will know, 2009 is the International Year of Astronomy (IYA). Many public events are planned in 140 nations around the globe, to celebrate astronomy, to raise the awareness of the general public, and to engage students of all ages. The observatories on Mauna Kea in Hawaii are participating in many of the global events, and they also put on a few of their own. Some are annual events that have a special IYA theme this year, others are one-off events just for this year. JAC's UKIRT and JCMT staff are participating in all of these.

A full report and photographs of these activities appear in the similarly-titled article on page 14 of the Spring 2009 issue of the *JCMT Newsletter*. Additional photographs appear on the rear cover of this *Newsletter*.

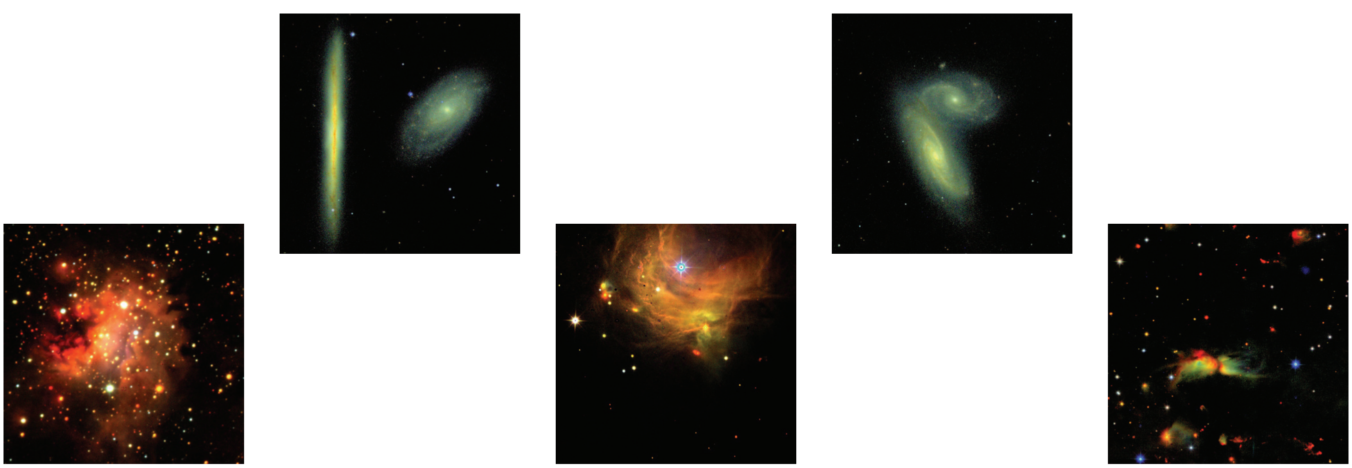

Figure 1. — Mosaic images from the WFCAM Science Archive (Edinburgh).

Brown Dwarfs and UKIRT: From Speculation to Observations to Classification

Sandy Leggett & Tom Geballe (*Gemini*)

Brown dwarfs are compact star-like objects that have total masses less than 7% of the Sun, or equivalently less than 75 Jupiter masses. After forming from the molecular cloud, they cool and collapse down to the size of Jupiter over a period of about 300 Myr. Electron degeneracy in the core prevents the dwarf from collapsing further and also prevents the core from heating up to the temperature required to fuse hydrogen. Hence, unlike stars, brown dwarfs never reach a long-lived period of constant luminosity, but instead slowly cool and fade away. (The term "brown dwarf" was coined in the 1970s and has stuck, although recent modellers describe their colour as more maroon-like!)

In 1963, the existence of brown dwarfs was proposed independently by two groups, Hayashi & Nakano (1963) and Kumar (1963). The search began for objects cooler than the coolest stars known at that time, the M dwarfs. M dwarfs range in mass from about half a solar mass down to the brown dwarf upper limit, and have surface temperatures from 3800 K at the massive end to 2200 K at the low-mass end. The adopted letters for the low-temperature extension of the main-sequence are L, followed by T, followed most likely by Y (Kirkpatrick et al. 1999).

The L dwarfs have masses <~ 80 Jupiters and temperatures of 2200 K to 1300 K — the earliest-type L dwarfs can be stellar; *i.e.*, they may not be brown dwarfs. The T dwarfs are necessarily "brown" with masses <~70 Jupiters. They are cooler than 1300 K; just how cool they can be is unknown. All dwarfs cooler than about 3000 K and older than about 300 Myr have a radius equal to that of Jupiter, or one-tenth that of the Sun. Their low temperatures and small surface area mean that cool dwarfs are faint, and are easiest to find in the solar neighbourhood.

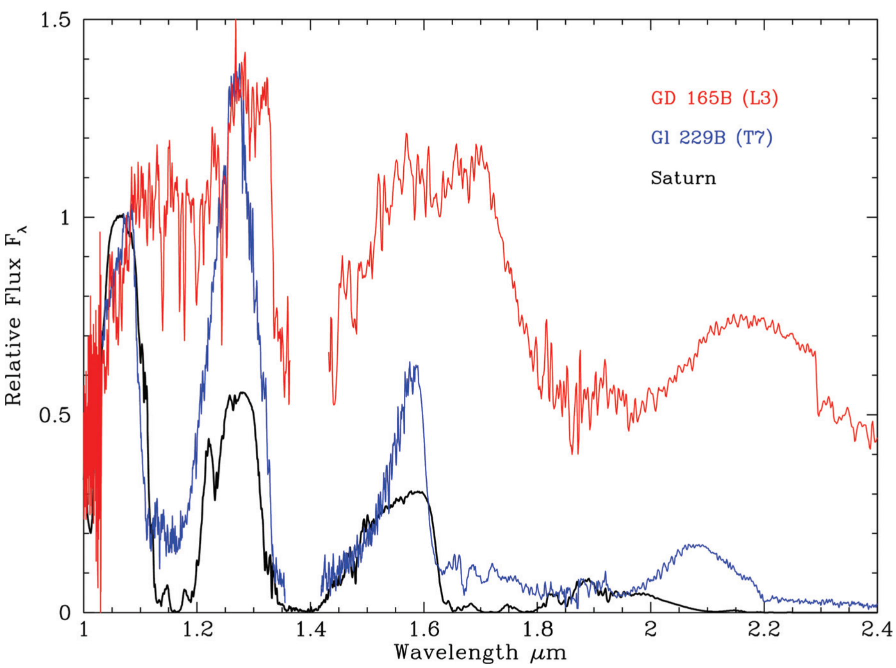

Figure 1. — CGS4 spectra of Saturn and the prototype L and T dwarfs GD 165B and GL 229B (Geballe et al. 1996 and unpublished; Leggett et al. 2001). The T dwarf looks very similar to Saturn; in particular, both the planet and the T dwarf have a strong methane absorption feature around 1.6 μm.

The very latest-type and coolest M dwarfs were predominantly found as a result of large-scale proper motion studies which started in the 1950s. Initial searches for the objects beyond M dwarfs either looked for objects redder than M dwarfs, or for faint objects with high proper motions (which would suggest that they were nearby and thus intrinsically faint), or imaged stars and white dwarfs for low-luminosity companions.

It took many decades to find examples of objects significantly cooler than M dwarfs. Although only classified as such later, the prototype L and T dwarfs were both discovered as companions: the first L dwarf, GD 165B, was discovered as a companion to a white dwarf in 1988 (Becklin & Zuckerman 1988), and the first T, GL 229B, as a companion to an M dwarf in 1995 (Nakajima et al. 1995). Although the spectrum of GD 165B looks like an extreme example of an M dwarf, the spectrum of GL 229B looks totally different and planet-like, because it shows strong methane absorption bands.

The discovery of GL 229B marked a true frontier in stellar astronomy, and observational and theoretical studies of brown dwarfs, objects connecting the stars to the planets, began in earnest.

A low-resolution infrared spectrum of GL 229B was published in 1995, but the subsequent higher resolution and higher quality CGS4 spectrum obtained at UKIRT in 1995 (Geballe et al. 1996) became the definitive measurement (Figure 1). This spectrum showed a large number of water and methane absorption lines, and Geballe et al. could demonstrate its similarity to CGS4

(Brown Dwarfs, continued on page 6)

(Brown Dwarfs, continued from page 5)

spectra of Saturn and Titan.

Later, dwarfs with near-infrared methane features would become known as T-type dwarfs. Pioneering work on GL 229B using CGS4 continued at UKIRT with the initially surprising discovery of significant CO absorption at 5 μm (Noll et al. 1997). At the ~1000 K temperature of GL 229B, all carbon in the photosphere should be in the form of methane, and CO should be an undetectable trace species. However, as Noll et al. pointed out, mixing occurs in the upper atmosphere, with CO being dredged up from lower layers where it is more abundant (as also occurs in Jupiter). In the photosphere of GL 229B the amount of CO is enhanced by a factor >1000 and the effect at wavelengths near 5 μm is huge: the dwarf is about a factor of two fainter than expected.

The year 1997 marked the start of the discovery of the L dwarf population. Initial discoveries from the Two Micron All Sky Survey (2MASS, Skrutskie et al. 2006) included a number of extremely red objects, including one object recognised by Kirkpatrick et al. (1997) as requiring a type beyond the M class. In the same year Ruiz et al. (1997) used IRCAM and CGS4, together with ESO optical instrumentation, to show that a newly discovered high proper motion object was the third example of this class, now known as L dwarfs.

In 1999, the 2MASS and Deep Near-Infrared Survey (DENIS, Epchtein et al. 1997) would publish tens of L dwarfs, together with a definition of their optical classification. (For a brief time, the mnemonic for the star classification sequence OBAFGKM "oh be a fine guy/girl, kiss me" was altered to include the L at the end by incorporating "Bill" and "Monica Lewinsky"!) In 2000, CGS4 was used to demonstrate that the L dwarfs show methane absorption at 3 μm (Noll et al. 2000). This marked the highest temperature appearance of methane in the star to brown dwarf spectral sequence.

Meanwhile, the search for other GL 229B-like objects, cooler dwarfs which show methane in their near-infrared spectra, had been continuing unabated. However, it was not until 1999 and the start of a collaboration between the Sloan Digital Sky Survey (SDSS, York et al. 2000) and Geballe and Leggett using UKIRT, that another example was found. SDSS team member Knapp contacted Geballe to arrange followup in the near-infrared of a uniquely red object found in the SDSS commissioning data. Geballe had recently moved to Gemini, but contacted Leggett. Together they used IRCAM and CGS4 in April and May 1999 to confirm the second example of a T-type brown dwarf (Strauss et al. 1999).

Additional T dwarfs were found later that year by both SDSS and 2MASS. Strangely, the first six objects appeared to be almost identical to GL 229B, leaving a gap between the L dwarfs — with no methane in the near-infrared, and the known T dwarfs — with pronounced methane features. In March of the following year, several "missing links" were found during a single very exciting night at UKIRT, with Leggett, Knapp, and Geballe all present. CGS4 was used to confirm three early-type T dwarfs with steadily strengthening methane bands at 1.6 and 2.2 μm (Figure 2; Leggett et al. 2000). As a result of that night an entire new spectral class could finally be defined.

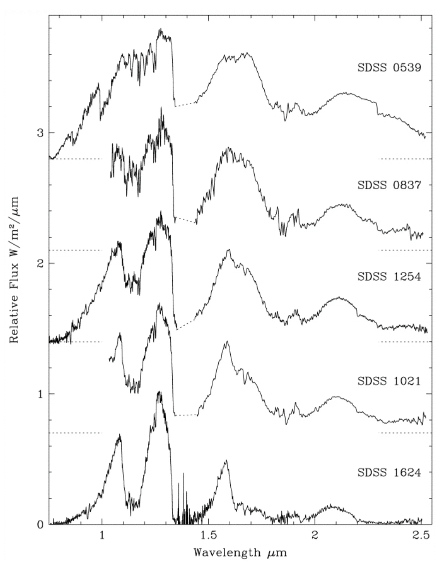

Figure 2. — CGS4 observations showing the T-dwarf spectral sequence (from Leggett et al. 2000). The three early T dwarfs (SDSS 0837, SDSS 1254, and SDSS 1021) are ordered by increasing CH_4 absorption. A later T dwarf (SDSS 1624) and an L dwarf (SDSS 0539, ~L5) are also plotted for comparison.

The SDSS–UKIRT collaboration would continue to be extremely productive for the next six years, producing heavily cited publications. CGS4 data contributed significantly to the universally adopted classification scheme for T dwarfs (Geballe et al. 2002, Burgasser et al. 2006). CGS4, IRCAM, UFTI and UIST data were used by Knapp et al. (2004) in a much-cited study of the effects of temperature, condensate clouds and gravity on L and T dwarfs. In particular, Knapp et al. showed that the marked change in near-infrared color between the L and T dwarfs could be explained by a rapid increase in grain sedimentation at almost constant temperature. (Within our group the phenomenon is referred to as the "Hilo rain" scenario.) Golimowski et al. (2004) used IRCAM and UIST to obtain 3–5 μm *L*' and *M*' photometry of L and T dwarfs (Figure 3). These data confirmed that CO enhancement, or nonequilibrium chemistry, is a common feature of brown dwarf atmospheres. The data were also used to obtain bolometric luminosities to derive an accurate temperature sequence for the low-temperature end of the main sequence; this remains the com-

(Brown Dwarfs, continued on page 7)

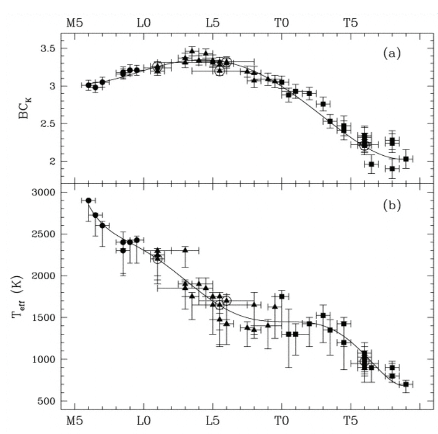

Figure 3. — Diagrams of (upper panel) BC_K and (lower panel) T_{eff} (mean age 3 Gyr) plotted against spectral type for ultracool dwarfs. The curves are polynomial fits to the data. See Golimowski et al. 2004 for further details.

H_3^+ at UKIRT — A Saga of Discovery

Tom Geballe (*Gemini*)

In 1981, about the time I was moving from the Carnegie Institution in Pasadena to UKIRT in Hilo, I received a phone call from Professor Takeshi Oka of the Departments of Chemistry and Astronomy at the University of Chicago, a man I had neither met nor knew of. He asked if I would help him search dense interstellar clouds for the molecular ion H_3^+, a substance I also had never heard of and the astrophysical significance of which I obviously was completely unaware.

Oka clearly had a deep knowledge of chemistry and physics, but little experience in observational infrared astronomy. He had gotten my name from my graduate advisor, Prof. Charles H. Townes, from whom I had received my Ph.D. in physics at Berkeley seven years earlier. I was not all that experienced either, but I had helped to build several infrared spectrographs for astronomy. One of them had just been used by graduate student Daniel Nadeau, his advisor, Prof. Gerry Neugebauer of Caltech, and me to make some significant discoveries about the nature of the recently detected shock-excited molecular hydrogen (H_2) in the Orion Molecular Cloud.

Oka's enthusiasm was such that despite my ignorance of H_3^+ there was no way I could turn him down. He had succeeded where others had failed in measuring the infrared spectrum of H_3^+ in the laboratory and was now eager to detect it in space. Indeed he had already attempted to do so at Kitt Peak National Observatory, but his attempt had been, in his words, a "miserable failure."

After a little investigation, the significance of H_3^+ in astronomy began to become apparent to me. H_3^+, an equilateral triangular arrangement of three protons, with two orbiting electrons, is the catalyst for nearly all of interstellar gas phase chemistry. Formed by the cosmic ray induced ionization of H_2 (the dominant species in molecular clouds) followed by the ion-molecule reaction, $H_2^+ + H_2 \rightarrow H_3^+ + H$, the newly created H_3^+ will gladly donates its spare proton to nearly any other neutral atom or molecule it encounters. The receiver of the proton then itself becomes highly reactive. Neutral-neutral chemistry is exceedingly slow in the low temperature environment of dark clouds, but ion-molecule reactions that include such proton hops are rapid and the reaction rates are nearly insensitive to temperature. Hence one can envision interstellar gas phase chemistry as a network of ion-molecule reactions that starts with the creation of H_3^+. Most of the molecular species that we observe in dense clouds, including CO, H_2O, H_2CO, NH_3, CH_4, and a number of cyanopolyynes such as HC_5N, HC_7N, and HC_7N that Oka and his collaborators had recently discovered using radio telescopes, are created in this way.

Ion-molecule chemistry as the dominant chemistry in molecular clouds had been proposed in the 1970s, and the idea had been quickly accepted. But H_3^+, its smoking gun, had not been detected. Presumably it was rare. Yes, it was being created at a good clip; a typical hydrogen molecule in a typical dark cloud — 0.1 parsec in extent and containing maybe 3×10^{56} H_2 molecules —

(H_3^+, continued on page 8)

(Brown Dwarfs, continued from page 6)

monly used temperature scale.

UKIRT remains at the forefront of brown dwarf discoveries, due to the ongoing contributions of the UKIRT Infrared Deep Sky Survey (UKIDSS, Lawrence et al. 2007). This survey, in particular the Large Area Survey (LAS) component, is extending the population of brown dwarfs found by 2MASS and SDSS to fainter, more distant, and cooler, objects. Already, with the results of less than a quarter of the survey published, UKIDSS T dwarfs make up more than 20% of the known number of such objects (*e.g.*, Pinfield et al. 2008); UKIDSS will find more T dwarfs than 2MASS and SDSS combined.

The LAS has also discovered what appears to be the coolest dwarf currently known: ULAS 1335+1130, with a surface temperature of between 500 K and 550 K (Burningham et al. 2008, Leggett et al. 2009). This object still spectrally appears T-like, but there are hints of ammonia in the near-infrared spectrum, and we may be at the brink of discovering the Y class dwarfs, cold objects much more similar to planets than stars. Interestingly, the number of known T dwarfs is currently only 153 (see, *e.g.*, `http://dwarfarchives.org/`), and is less than the number of known extrasolar planets (there are 228 according to `http://exoplanets.org/`); we expect that UKIDSS will remedy this situation. UKIDSS also has a good chance of finding the first Y dwarf. That discovery will mark the next frontier in this exciting field, to which UKIRT has already contributed so much.

Referenes

Becklin, E. & Zuckerman, B. 1988, *Nature*, 336, 656.
Burgasser, A. et al. 2006, *ApJ*, 637, 1067.
Burningham, B. et al. 2008, *MNRAS*, 391, 320.
Epchtein, N. et al. 1997, *Msngr*, 87, 27.
Geballe, T. et al. 1996, *ApJ*, 467, L101.
Geballe, T. et al. 2002, *ApJ*, 564, 466 .
Golimowski, D. et al. 2004, AJ, 127, 3516.
Hayashi, C. & Nakano, T. 1963, *Progress of Theoretical Physics*, 30, 460.
Kirkpatrick, D. et al. 1997, *ApJ*, 476, 311.
Kirkpatrick, D. et al. 1999, *ApJ*, 519, 802.
Knapp, G. et al. 2004, *AJ*, 127, 3553.
Kumar, S. 1963, *ApJ* 137, 1121.
Lawrence, A. et al. 2007, *MNRAS* 379, 1599.
Leggett, S. et al. 2000, *ApJ*, 536, L35.
Leggett, S. et al. 2001, *ApJ* 548, 908.
Leggett, S. et al. 2009, *ApJ* in press (*arXiv*: 0901.4093) .
Nakajima, T. et al. 1995, *Nature*, 378, 463.
Noll, K. et al. 1997, *ApJ*, 489, L87.
Noll, K. et al. 2000, *ApJ*, 541, L75.
Pinfield, D. et al. 2008, *MNRAS*, 390, 304.
Ruiz, M. et al. 1997, *ApJ*, 491, L107.
Skrutskie, M. et al. 2006, *AJ*, 131, 1163 .
Strauss, M. et al. 1999, *ApJ*, 522, L61.
York, D. et al. 2000, *AJ*, 120, 1579.

(H_3^+, continued from page 7)

had to wait "only" about a billion years, 3×10^{16} s, to be ionized by the cosmic ray background. Because it is the rate at which this ionization occurs that controls the production of H_3^+, the rate of total production in such a cloud is simply the ratio of those two numbers. Thus, about 10^{40} H_3^+ molecules would be created in the cloud each second. This seems like an astoundingly large rate and it seems that the process should produce an even more astoundingly large total number of H_3^+ molecules in the cloud, and it does. But H_3^+ is highly reactive; it destroys itself any time it bumps into just about anything other than hydrogen or helium. So even though that total number is huge, the cloud is vast and the steady state concentration of H_3^+ in it is predicted to be relatively low, typically a few parts per billion. This meant that the spectroscopic signature of H_3^+ likely would be very faint.

As I pondered how to best search for H_3^+, whose strongest transitions are in its fundamental asymmetric stretching (vibrational) band in the 3–4 μm region, a strategy soon emerged: perform absorption spectroscopy of a dense molecular cloud using as a light source, an infrared-bright young stellar object in or perhaps behind the cloud. The two requirements (in addition to a good infrared telescope on a good infrared site) were a sensitive high-resolution spectrograph capable of measuring weak and narrow absorption lines at those wavelengths, and a sufficiently bright stellar object to provide a high signal-to-noise ratio. Together these might make it possible to detect the expected weak lines of H_3^+. Unfortunately both were in short supply. UKIRT was not due to receive such an instrument for a few years, no other sensitive 3–4 μm spectrograph existed on Mauna Kea, and based on the expected sensitivity at UKIRT of the new instrument (a combination cold grating and warm Fabry-Perot spectrometer) one could count the sufficiently bright and suitable embedded stellar sources on the fingers of one's hands.

When the aforementioned spectrometer became available at UKIRT, Oka and I successfully applied for observing time. During the mid and late 1980s we made a few attempts to detect H_3^+, all of which were unsuccessful. Some of the upper limits to the abundance of H_3^+ that we obtained were close to the predicted values and in one cloud a faint and almost believable signature of H_3^+ was present. But it was clear that, assuming that ours was the best observing strategy, significant improvement would require the next generation of infrared spectrometers.

At about the time Oka's and my paper reporting these negative results appeared in the literature, news came of the exciting and totally unexpected discovery, made at the Canada–France–Hawaii Telescope, that the H_3^+ overtone band at 2 μm produces bright high altitude aurorae at the poles of Jupiter. For the moment the two of us set aside our interest in the interstellar medium in order to follow up at UKIRT on this first detection of H_3^+ outside the laboratory. On several mornings during September of 1989, after the night's observers departed, we successfully sought and measured many fundamental band lines of H_3^+ in Jupiter.

These observations, which we published in 1990, are a rare example of daytime science done at UKIRT. I recall that each morning as Oka and I took over the telescope, the seeing was excellent. However, a little over an hour after we had started to observe the entire dome and telescope, and the observers, would begin to shake. The construction crew build-

(H_3^+, continued on page 9)

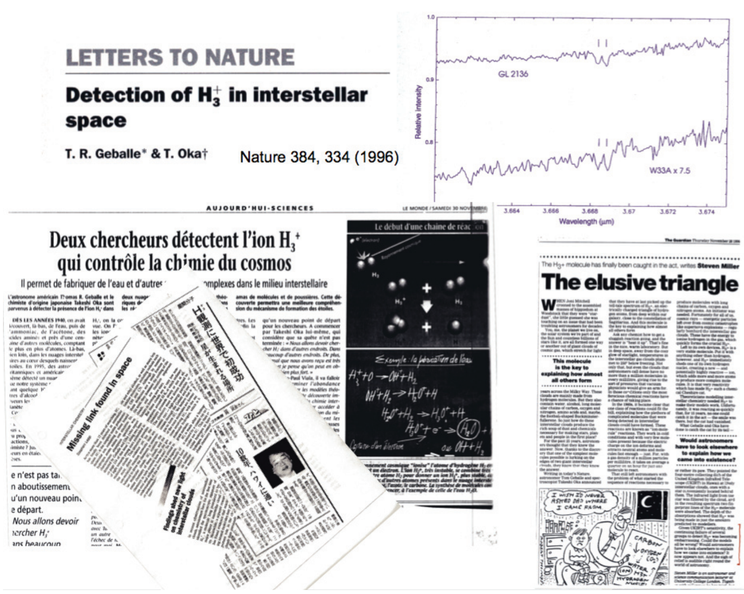

Figure 1. — At top left is part of the title page of the discovery paper published in Nature on 28 November 1996. At top right are the spectra of the two molecular clouds from July 15, 1996 that clinched the detection of H_3^+. The predicted wavelengths of the absorptions in each cloud are indicated by the short vertical lines. At bottom is some of the reaction of the world press.

(H_3^+, continued from page 8)
ing the paved road connecting the summit road and the NASA and Keck telescopes had arrived and had started its work; the crew was excavating directly down the hill from UKIRT! We persevered through that until a little after 8:00 a.m., when the seeing would suddenly degrade to a few arc seconds, presumably due to the onset of ground layer turbulence in the air surrounding the telescope, caused by the heating of the loose lava on the summit. Our view of Jupiter became very blurry. That change brought an end to each morning's observing.

We were excited to finally be seeing H_3^+ in space. Our observations showed that the lines of the fundamental band of H_3^+ were impressively strong in Jupiter's hydrogen-rich atmosphere and that, although brightest very close to the poles, they were also present elsewhere. Within a few years we and our collaborators, in particular Steve Miller of University College London and Laurence Trafton of the University of Texas, now using the newly arrived and revolutionary two-dimensional (58×62) array spectrometer, CGS4, were able to show that the Jovian H_3^+ line emission extended across the entire planet. We also discovered that on Uranus H_3^+ line emission also is present across the entire planet and that Saturn possesses prominent H_3^+ aurorae. We did not succeed in detecting H_3^+ on Neptune, and nobody else has succeeded to date.

By then it was the mid-1990s and Oka's and my attention turned back to the interstellar medium and the hunt for H_3^+ in dense clouds. The next generation of sensitive high-resolution infrared spectrographs on Mauna Kea was here, in the form of CGS4 at UKIRT and CSHELL at the NASA Infrared Telescope Facility (IRTF). At the time the spectral resolution achievable with CSHELL was 2–3× higher than CGS4. Although we were obviously quite familiar with UKIRT and CGS4 (and I was by then Head of Operations), we were concerned that CGS4's spectral resolution was not nearly high enough to be optimal for detection of the expected weak and narrow lines of interstellar H_3^+. Therefore in autumn 1994 we applied for observing time at the IRTF. Our proposal was rejected. The same thing happened the following semester. Along with the rejections came some suggestions from the time allocation committee of how we might improve our proposal. The next semester we submitted what we believed was an improved proposal. To our dismay we were turned down a third time.

Meanwhile, at UKIRT CGS4 was undergoing an upgrade to its current 256×256 array. The new array had much smaller pixels, giving CGS4 the capability of matching CSHELL in spectral resolution. Although we had missed the most recent semester deadline for UKIRT proposals, I knew that there was a mechanism for quickly obtaining a small amount of observing time, the UKIRT Service program. It had also become clear to me that due to the cold, high, and usually dry atmosphere above Mauna Kea, we could probably make a better choice of lines to initially seek; a close pair of H_3^+ lines near 3.67 μm should give us a somewhat better chance for detection than the single slightly stronger line at 3.95 μm that we had used in our earlier searches. Soon our proposal for a couple of hours of Service time to search for H_3^+ in two dense clouds was accepted and on April 29, 1996 I found myself at UKIRT as the scheduled (by me!) observer on a Service night.

Late that night, within a few minutes of beginning the observation of the first cloud, I could see the evidence for H_3^+ in the form of two weak but apparently real absorption lines. Within another hour the second cloud showed a somewhat more convincing detection. I excitedly emailed Oka the news. We decided to be cautious. Two and one-half months later, on July 15, we repeated the observations, using as a convenient test the changing Doppler shift of the lines caused by the orbital motion of the earth around the sun. The lines were there again, more clearly than in April and slightly shifted in wavelength, just as expected (see Figure 1). Analysis showed that the amount of H_3^+ we had detected was consistent with that predicted from the ion molecule chemical model. The smoking gun had been detected and the viability of the ion-molecule model was confirmed. By the end of November we had published a Letter in the journal *Nature* announcing this. As can be seen in Figure 1, we experienced our fifteen minutes of fame. It had been fifteen years since we started on our quest.

This is only a part of the story of H_3^+ at UKIRT, the telescope at the center of my career as an astronomer, and the JAC, an observatory whose uniquely supportive staff, past and present, remains dear to my heart. UKIRT has played the seminal role in both the discovery and exploration of H_3^+ in the interstellar medium, as well as contributing enormously, via initial detections and detailed investigations, to our understanding of H_3^+ in the gas giant planets of the outer solar system. As of the end of 2008 Oka and I together with our collaborators had published more than twenty refereed papers on H_3^+ based entirely or in part on observations made at UKIRT. (There are still a few more papers in our heads, waiting to be written.) In addition to the initial detection of interstellar H_3^+ and the initial detections on Uranus and Saturn, the unexpected discovery that H_3^+ is abundant in the diffuse interstellar medium, a finding that has had far reaching implications, occurred at UKIRT. It also should be noted that the first detection of H_3^+ in the interstellar medium of an external galaxy was made at UKIRT.

Many key questions involving the astrophysics of H_3^+ require telescopes larger than UKIRT for answers. However, there remains plenty of important H_3^+ science for 4-meter class telescopes. Should UKIRT's excellent Cassegrain spectrographs return to action, Oka and I will happily and eagerly request to use them to continue our research.

Unravelling Post-AGB stars in the Infrared with UKIRT

Tim Gledhill (*Hertfordshire*)

UKIRT provides a unique opportunity to astronomers in that it offers polarimetric capabilities with all of its infrared Cassegrain instruments. High precision polarimetry became a routine operation with the commissioning of the IRPOL2 rotating waveplate module in 1995 which, in conjunction with beam-splitting or wire-grid analysers, has allowed imaging and spectro-polarimetry in the near- and mid-infrared. A further strength is the range of astronomical techniques covered at UKIRT (such as imaging, long-slit and integral field spectroscopy) and the ease with which modes can be interchanged during the night, all controlled by the same software acquisition system and data-reduction pipeline.

From the point of view of post-AGB work, the ability to combine imaging polarimetry and integral field spectroscopy is particularly attractive.

The late stages of stellar evolution are characterised by prodigious mass loss, particularly on the Asymptotic Giant Branch (AGB), resulting in the formation of a circumstellar envelope of molecular gas and dust. In this way, the majority of stars in the Galaxy will shed their excess mass, allowing the remnant cores to evolve to become white dwarfs, some of which will briefly be the central stars of planetary nebulae. Imaging polarimetry may be used to investigate the structure and density of these dusty envelopes, providing clues to the evolution of the mass-loss process along the AGB — a vital ingredient in stellar evolution models.

HD 179821 is one such evolved star, surrounded by a dusty envelope which is seen at optical and infrared wavelengths as scattered light. In Figure 1 a HST planetary camera image (Ueta et al. 2000) shows an extended shell around the central bright star, with clear evidence for collimated outflows in the form of radial plumes. The overlayed vectors show the linear polarization throughout the shell in the *J*-band, obtained at UKIRT in 1998 using the now-retired IRCAM/TUFTI detector (Gledhill et al. 2001). The polarimetic imaging demonstrated that the outflow is well described by a detached shell with a r^{-2} radial density fall-off, suggesting that the mass-loss rate was fairly constant before dropping dramatically.

The intrinsic polarization in the HD 179821 dust shell (after correction for the bright PSF of the central star) is 30–40%. Scattering models show that these high degrees of polarization, combined with a small infrared colour excess, may require the presence of fluffy or aggregate dust particles in the envelope around this star (Gledhill & Takami 2001). The plumes appear to be more recent collimated outflows that are now interacting with and disrupting the circumstellar shell.

Ground-based polarimetry can be used as a fast and efficient technique for the detection of extended scattering envelopes around mass-losing evolved stars. The polarimetry allows the separation of the polarised circumstellar envelope from the unpolarized PSF, overcoming the problem of imaging faint material close to a bright star. This technique is sometimes referred to as "polarimetric differential imaging", a slightly tautological description as polarimetry is inherently a differential technique.

In Figure 2 the post-AGB star IRAS 06530–0213 is shown in both total and polarised intensity in the *J*-band. The total intensity image (Stokes *I*) is dominated by the PSF of the central

(Post-AGB Stars, continued on page 11)

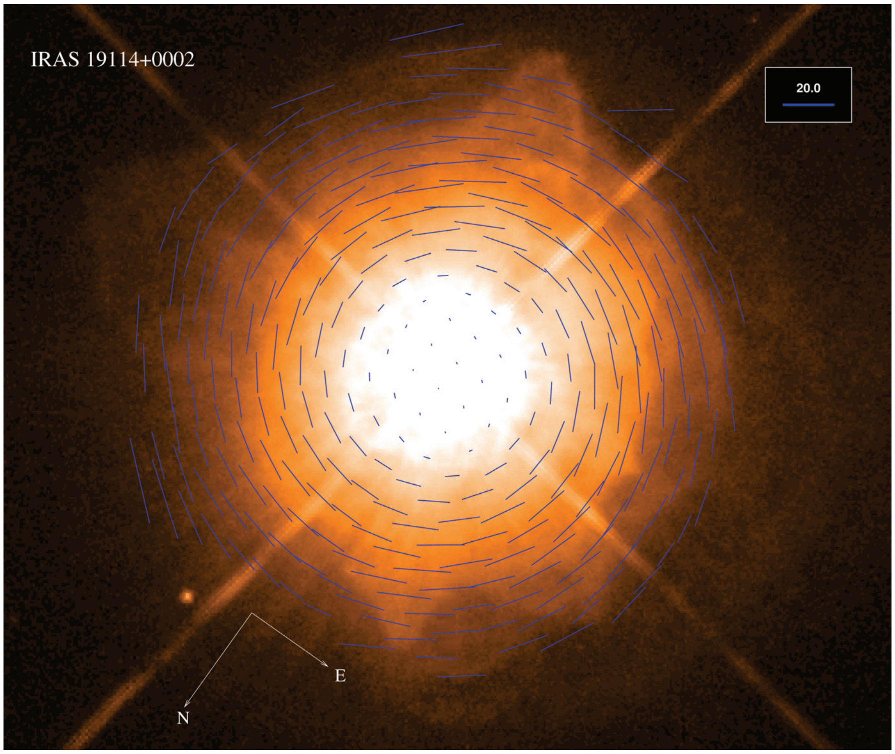

Figure 1. — HD 179821 imaged with WFPC2 aboard HST using a wide-band F555W (roughly V-band) filter. The dimensions of the image are approximately 12×12" and a logarithmic scaling is used. The overlayed J-band polarization vectors were obtained using IRCAM/TUFTI on UKIRT and show high degrees of linear polarization (up to 40% after correction for the stellar PSF) due to light scattering in the circumstellar dust shell.

(Post-AGB Stars, continued from page 10)

bright star, although the overlayed polarization vectors indicate the presence of a scattering dust envelope. In linear polarized intensity, the unpolarized stellar PSF disappears revealing an axisymmetric dust shell around the star. In this way the circumstellar environments of over 50 post-AGB stars have been studied, revealing a range of morphologies, from mildly asymmetric shells to highly collimated bipolar outflows with dense circumstellar discs (Gledhill 2005). One common factor seems to be that, by the post-AGB stage, mass-loss has become non-spherically symmetric to some degree. The origin of this non-sphericity is a topic of debate, but it seems likely that a binary companion must be involved, at least in the cases of the most highly bipolar outflows. This has now been confirmed in a number of objects, for example in the famous Red Rectangle nebula (van Winckel et al. 1995; Witt et al. 2009).

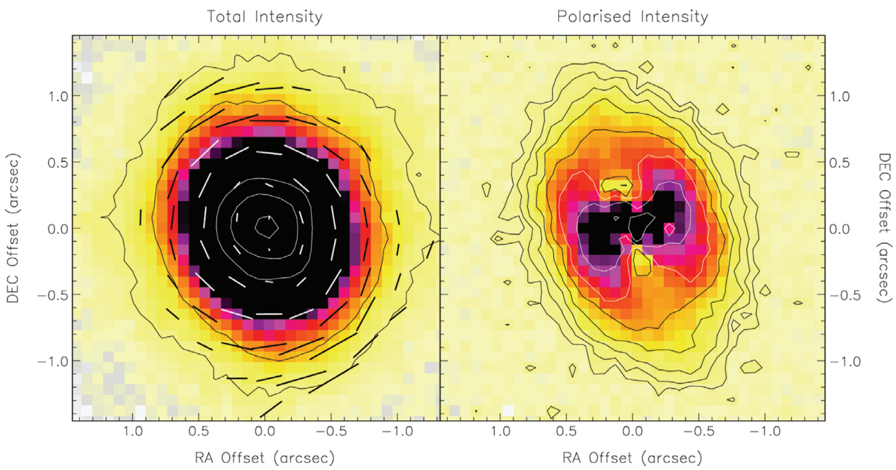

Figure 2. — The post-AGB object IRAS 06530-0213 in both (left panel) total and (right panel) linearly polarized intensity. The total intensity image is dominated by the bright stellar PSF, which is effectively removed when the object is viewed in polarized light, revealing an axisymmetric dust shell around the star. The images were obtained using UIST.

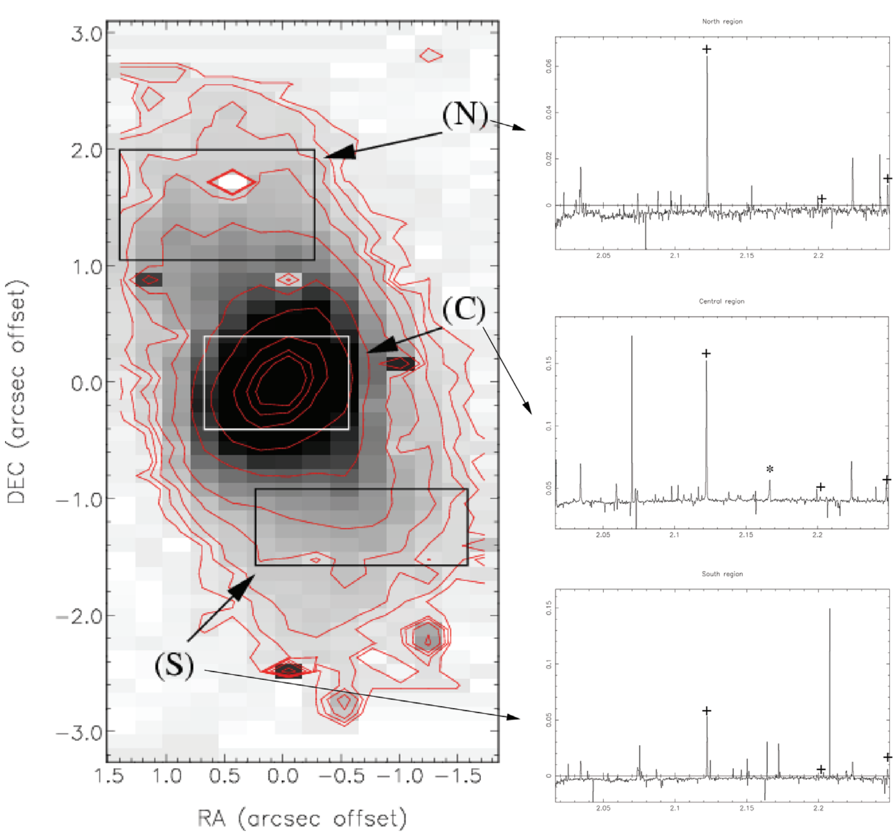

Figure 3. — (left panel) A continuum-subtracted image of the young planetary nebula IRAS 19306+1407 in the H_2 1-0 S(1) line at 2.122 µm, obtained using the IFU mode of UIST. The integral field mode allows H_2 emission lines to be mapped over the extent of the outflow. (right panels) Sample spectra, extracted from various locations in the data-cube, are shown.

The environments of post-AGB stars are largely molecular, even into the early planetary nebula phase, and the ro-vibrational lines of H_2 can be used to trace the gas content in the outflows. In particular, the IFU of UIST enables H_2 emission to be mapped over the extent of any outflow, providing information on the gas excitation and kinematics. As fast winds begin to blow in the post-AGB phase, sculpting and forming the emerging planetary nebula, H_2 emission from shocks as well as from fluorescence due to the increasing stellar UV emission, is observed.

Figure 3 shows contours of the continuum-subtracted 1-0 S(1) line at 2.122 µm, in the post-AGB object IRAS 19306+1407, overlayed on a *K*-band continuum image (Lowe 2008). The elongated H_2 emission arises in a bipolar outflow from the star and is largely shock-excited. Modelling of the line strengths and ratios allows the details of the excitation mechanisms to be explored. The power of these techniques, however, comes from combining the polarimetry and the IFU measurements to provide a picture of the dust and gas outflows in these sources and the way in which the two interact to shape and form planetary nebulae.

References

Gledhill, 2005, *MNRAS*, 356, 883.
Gledhill, Chrysostomou, Hough & Yates, 2001, *MNRAS*, 322, 321.
Gledhill & Takami, 2001, *MNRAS*, 328, 266.
Lowe, 2008, *Ph.D. Thesis*, University of Herfordshire.
Ueta, Meixner & Bobrowsky, 2000, *ApJ*, 528, 861.
van Winckel, Waelkens & Waters, 1995, *A&A*, 293 L23.
Witt et al., 2009, *Apj* in press, *arXiv*:0812.2893.

UFTI Observations of Transiting Extrasolar Planets

Ernst de Mooij & Ignas Snellen (*Leiden*)

Radial velocity searches for transiting extrasolar planets are responsible for the majority of the ~300 known exoplanet systems. Although these observations allow the statistics of planetary orbits and lower limits to planetary masses to be studied, it does not give information on the intrinsic properties of the planets, *e.g.*, size, density and atmospheric composition. The ~50 known *transiting planet systems* on the other hand do allow for measurement of these important properties.

From the transit lightcurve, the ratio of planet-to-star radii can be measured, which in combination with radial velocity measurements provides the radius and density, and subsequently an estimate of the internal structure of the planet. By observing the transit at different wavelengths, a direct measurement of the atmospheric properties can be made. In this way, recent observations have detected atoms and molecules (*e.g.*, sodium, water and methane) in the atmosphere of several exoplanets (Charbonneau et al. 2002, Snellen et al. 2008, Swain et al. 2008) and an evaporating hydrogen exosphere (Vidal-Madjar et al. 2003, 2004).

Observations of a secondary eclipse of a transiting planet — the moment a planet moves behind its star — give complementary information on the atmospheric properties. By measuring the planet-to-star contrast, the surface brightness can be determined. This gives information on the efficiency of absorption, reflection and reprocessing of the incident stellar light in the atmosphere of the planet.

Until recently all secondary eclipse measurements had been made from space, with the Spitzer Space Telescope (*e.g.*, Charbonneau et al. 2005, Deming et al. 2005, Knutsen et al. 2007) and the Hubble Space Telescope (Swain et al. 2009).

During the summer of 2008, we observed three different transiting exoplanets with the UKIRT Fast Track Imager (UFTI). Our goal was to obtain high accuracy measurements of their near-infrared radii. We also observed the secondary eclipse of one of the planets, to obtain a measurement of its thermal emission. A challenging aspect of observing most of the transiting exoplanet systems is that they are very bright, which prevents efficient observations, because most near-infrared instruments would saturate within a very short time scale. On the other hand, the bright transiting systems are needed to reach the high photometric precision required to detect the transit or secondary eclipse signal. For our observations, we therefore defocused the telescope to create a PSF of a few tens of pixels in diameter, corresponding to a few arcseconds. An example of such a defocused PSF can be found in Figure 1. By defocusing the telescope, and thereby spreading the light out over many pixels, we also reduced the effect of non-optimal flat fielding effects, the influence of hot and cold pixels, and possible intrapixel variations.

The first exoplanet system we observed with UKIRT was the TrES-3 system. The planet, TrES-3b, orbits its star in just 31 hr, at a distance of only 0.0226 AU (which corresponds to 6 $R_\odot$). Due to the very close-in orbit, the expected temperature of this planet is of the order of 2000 K, making it a very good target for measuring its thermal emission. The transit, which gives us information on the radius of the planet, was observed in June 2008. The measured radius in the near-infrared is 1.338±0.016 Jupiter radii. The observations, binned over nine points, are shown in the top panel of Figure 2.

The secondary eclipse of this planet was observed with UFTI one month later, although the observations suffered from rapidly changing seeing. This prevented us from using the data to measure the planets thermal emission. Fortunately, observations with the WHT on La Palma of the secondary eclipse of TrES-3b (Figure 2) have since resulted in a 6-sigma detection. This is the first ground-based detection of thermal emission from a hot Jupiter (de Mooij & Snellen 2009; though see also the observations of OGLE-TR-56b by Sing & Lopez-Morales (2009) in the same issue of A&A).

To measure the radius of HAT-P-1b, a hot-jupiter that transits its star approximately every 107 hr, we observed the transit of this planet in August 2008. Since HAT-P-1 is in a binary system with the second star located only 11" away, we decided to test an alternative dither pattern, using the second star as a reference. A sequence of four dither positions put both stars on different quadrants of the detector. The same dither pattern was repeated, but this time with the reference star centred in each quadrant. In subsequent cycles the places were switched again. In this way HAT-P-1 and the reference star were moved across

(Exoplanets, continued on page 13)

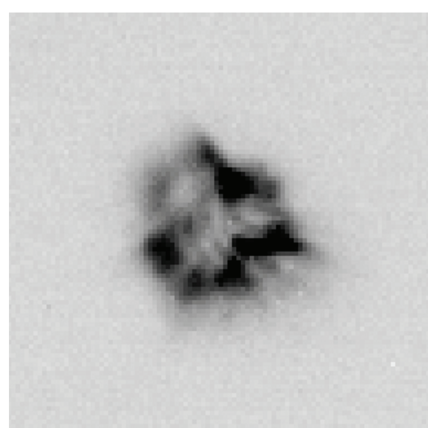

Figure 1. — An example of the PSF after defocusing the telescope.

(Exoplanets, continued from page 12)

many different positions on the chip. This meant that large scale structures in the flatfield significantly impacted the achieved precision. Spots of dust on the window of UFTI show up as bright spots in the data. We could therefore not use the *K*-band skyflats, and instead used a *J*-band flat to correct for sensitivity variations between pixels. Using this flat, the photometric precision significantly improved. This can be clearly seen in Figure 3, where we show the raw lightcurves flatfielded with a *J*-band flat and a *K*-band flat.

Although the analysis of the data is still ongoing, preliminary results show that the radius measured in the near-infrared is smaller than the radius measured at optical wavelengths. This indicates that the atmosphere of HAT-P-1b is more transparent at infrared wavelengths than at optical wavelengths.

Several important lessons can be learned from our observations. High accuracy flats are certainly vital, and shorter wavelengths may be used to correct for dust on the detector window. It is also clear from our observations of the secondary eclipse of TrES-3b that a stable PSF is quite important; large fluctuations in the seeing can impact the precision that is reached, probably because of detector non-linearity at very low, or very high, count levels. And, last but not least, it is clear that defocusing the telescope allows us to reach an extremely high photometric precision (~0.05 %/hr). With these caveats in mind, observations of the secondary eclipses of several other hot Jupiters are now possible.

References

Charbonneau et al. 2002 *ApJ* 568, 377.
Charbonneau et al. 2005 *ApJ*, 626, 523.
Deming et al. 2005 *Nature* , 434 , 740.
De Mooij & Snellen 2009 *A&A* 493, L35.
Knutson et al. 2007 *Nature* 447, 183.
Sing & Lopez-Morales 2009, *A&A* 493, L31.
Snellen et al. 2008, *A&A*, 487 357.
Swain et al. 2008, *Nature* 452, 329.
Swain et al. 2009, *ApJ* 690, L114.
Vidal-Madjar et al. 2003 *Nature* 422, 143.
Vidal-Madjar et al. 2004 *ApJ*, 604 L69.

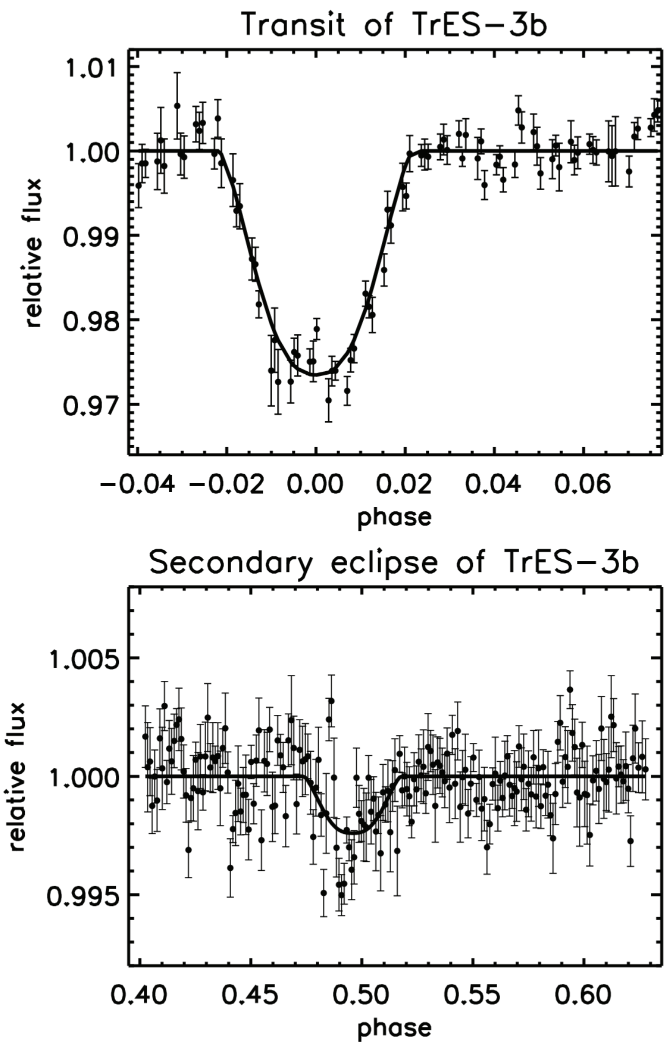

Figure 2. — (upper panel) Our UFTI observations of the transit of TrES-3b, binned over nine points. The solid line is the best fitting model. (lower panel) The secondary eclipse measurements of this planet obtained with the WHT on La Palma, again binned by 9 points. Note the order of magnitude difference in the measured depth between the transit (~2.7%) and the secondary eclipse (~0.24%) (de Mooij & Snellen 2009).

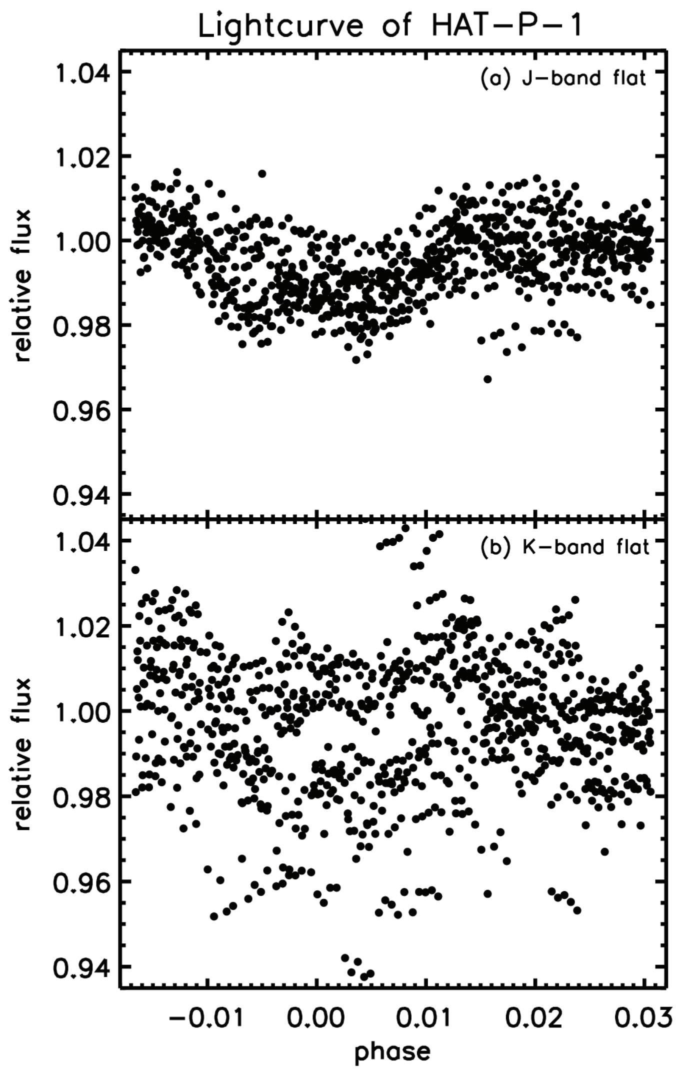

Figure 3. — A comparison between the photometry of the transit HAT-P-1b, with a (upper panel) J-band flat and a (lower panel) K-band flat. Note that the problems with the K-band flat noted in the text were enhanced by the fact that we used a non-regular dither pattern.

UKIRT and Subaru Observations of the Remarkable Braid Nebula Star Forming Region in Cygnus

Colin Aspin (*Hawaii*)

A region of active star formation that has been only poorly studied is the Lynds 1003 dark cloud in the Cygnus OB7 complex. Lying at around 800 pc, this region contains not one, but two young FU Ori-like variable stars. It also shows multiple signs of highly active star formation, with several Herbig-Haro (HH) flows, reflection nebulae, and infrared IRAS sources being present.

The region was first studied in detail by Movsessian et al. (2003, 2006). The complexity of the cloud, evident in these initial observations, suggested the need for further observations. We therefore formed an international collaboration of researchers at Institutes in Armenia (Tigran Magakian, Tigran Movsessian, Elena Nikogossian), Canada (Gerald Schieven), Ireland (Tigran Khanzadyan), Japan (Tae-Soo Pyo), the U.K. (Michael Smith, Sharon Mitchison), and the U.S. (Chris Davis, Tracy Beck), to study this region at multiple wavelengths and in multiple observing modes.

UKIRT has been integral to this study. So far, it has been used to obtain deep WFCAM images at *J*, *H*, *K*, and in narrow-band H_2. The Subaru Telescope was used to acquire complementary optical images at R, *I*, Hα, and [S II] to a similar depth. Figure 1 shows a sub-set of these images, focusing on the area around one of the FU Ori objects, named the Braid Nebula star after its remarkable twisted morphology in optical images. The Braid star itself can be seen as the bright nebulous object near the top-center of the *K*-band image. Papers on the optical and near-IR emission structures seen in the full images are currently in preparation (Magakian et al. 2009; Khanzadyan et al. 2009).

In addition to direct imaging, we

(Braid Nebula, continued on page 15)

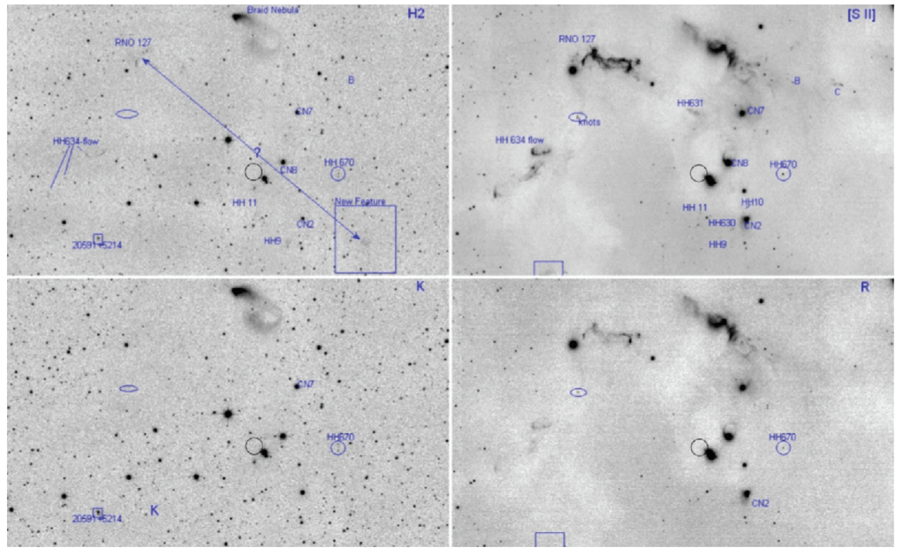

Figure 1. — Optical and near-IR images of a 20'×15' region of L 1003 containing the Braid Nebula. (upper-left panel) The WFCAM H_2 image, (upper-right panel) the Subaru [S II] image, (lower-left panel) the WFCAM K image, and (lower-right panel) the Subaru R image.

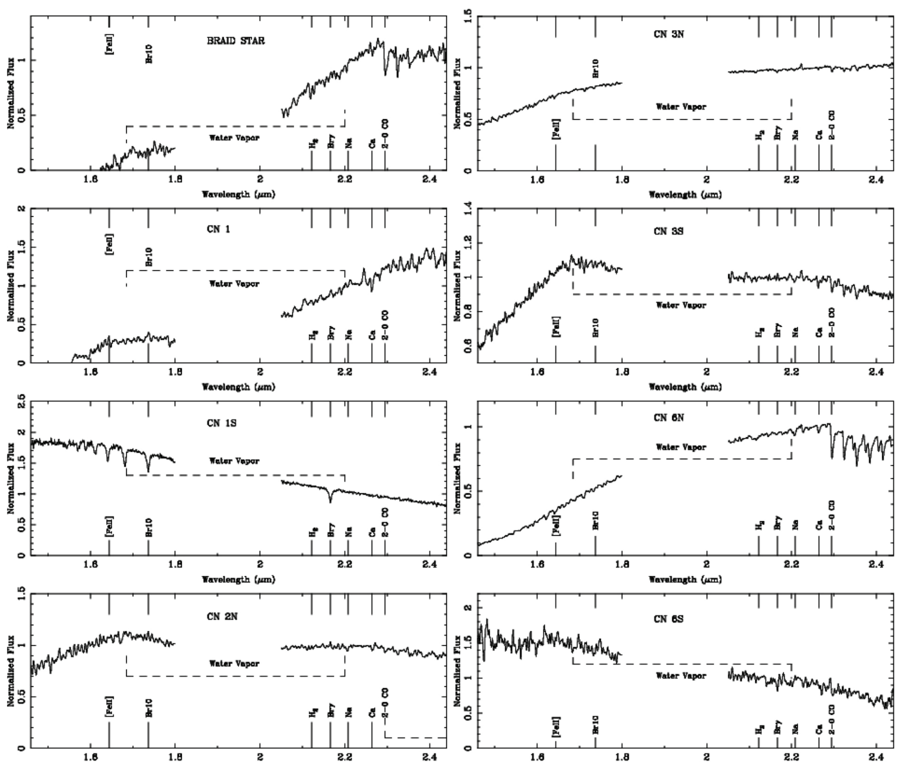

Figure 2. — UIST IFU HK-grism spectroscopy of just some of the young stars in the Braid Nebula region. A number of nebular emission and photospheric absorption features are labeled.

Inflow and Outflow from the Accretion Disc of the Microquasar SS 433

Sebastian Perez & Katherine Blundell (*Oxford*)

Microquasars are extraordinary objects which undergo the most extreme and efficient energy transformation process in the Universe: accretion onto a black hole!

SS 433 is probably the most exotic microquasar known so far. It became famous as the first known source of relativistic jets in the Galaxy, and is the only one known with baryonic content in its jets (see the comprehensive review by Fabrika 2004). Its jets are believed to emerge from an accretion disc, but direct evidence for this has thus far been scant.

In near-infrared spectra, SS 433 is characterised by the presence of numerous broad emission lines on top of a bright continuum originating from the accretion disc (McAlary & McLaren 1980; Thompson et al. 1979). As at optical and X-ray wavelengths, these emission lines can be divided into two groups: lines that are *stationary*, although highly variable in strength and profile shape, and lines that are *moving*. The latter are thought to originate in two oppositely-directed relativistic jets moving with a speed $v \sim 0.26c$.

Near-IR light can escape high opacity and dusty environments more easily than optical photons can. Telescopes like UKIRT are thus ideal for studying these heavily obscured line-emitting regions. Using data obtained with UIST, we have carried out a line de-blending procedure. The technique is based on fitting Gaussian profiles to near-IR spectra; we chose Brackett-γ (hereafter Br-γ), at a wavelength of 2.165 μm, as the most suitable emission line to model.

Decomposition of a line profile as the sum of Gaussian components is a technique widely used to extract information from different parcels of gas in a line-emitting region. For example, in the case of Seyfert galaxies it allows one to distinguish the "narrow line region" from the "broad line region" (*e.g.*, Ho et al. 1997). Blundell et al. (2008) decomposed the stationary Hα hydrogen line (observed during a quiescent period in SS 433's behaviour) into primarily 3 components: one broad component (implying gas moving at ~700 km/s) identified as the accretion disc wind, and two narrower, red- and blue-shifted components that are radiated from a glowing cir-

(SS 433, continued on page 16)

(Braid Nebula, continued from page 14)

subsequently obtained UIST near-IR IFU spectroscopy of 20 sources in the region. These data cover the *H* and *K* bands at a spectral resolution of about 1000. Our aim was to characterize the young stars in terms of spectral types, ages, masses, and activity level. Results from this study were published in Aspin et al. (2009). Figure 2 shows a composite plot of some of the data obtained, including observations of the Braid Nebula star itself.

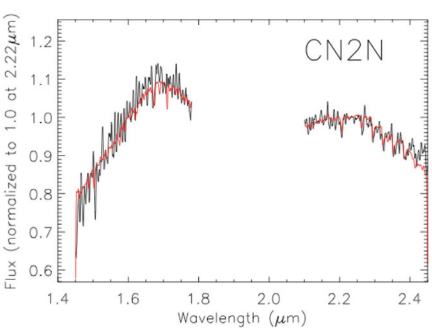

Figure 3. — Model fit to the continuum and photospheric absorption features seen in the HK spectrum of CN_2. The data are drawn in black; the fit is drawn in red.

The spectra reveal a wide variety of spectral structure. For example, the Braid Nebula star itself exhibits deep CO bandhead absorption longward of 2.294 μm, with little else present in its spectrum other than water vapor absorption.

We performed spectral template fitting of several of the young stars that possessed atomic and molecular absorption features, to obtain estimates of spectral type and other physical parameters, such as visual extinction, A_V, and *K*-band veiling, r_K. An example of the results of this fitting is shown in Figure 3. The best-fit spectral template for this source (CN_2 — seen lower-right of center in Figure 1 panels) gave values of spectral type M2(±2), A_V=12 (±2), and r_K=0.4(±0.3). In the Figure the fit to the spectrum is drawn in red, plotted over the observed data (which is drawn in black).

UKIRT is also being used to conduct photometric monitoring of the sources in the region. WFCAM *J*, *H*, and *K*-band images are being secured over the entire 0.8 deg^2 region centered on the Braid Nebula star. This project is on-going and we have so far obtained over 80 observations spanning a 2 yr period! The number of observations will eventually total around 120. Armed with these data we will perform an analysis of variability of the 100,000+ sources in the region. Due to the galactic longitude of L 1003 (approximately 90°) we are looking along a galactic spiral arm and hence many of these sources are background objects. Nonetheless, many new young variables, and hopefully some young eclipsing variables, will be found by this analysis, providing a wealth of sources for future follow-up observations. Stay tuned for results from this study in a future *Newsletter*.

References

Aspin et al. (2009) *AJ*, 137, 431.
Magakian et al. (2009) in prep.
Khanzadyan et al. (2009) in prep.
Movsessian et al., 2003, *A&A*, 412, 147.
Movsessian et al., 2006, *A&A*, 455, 1001.

(SS 433, continued from page 15)

cumbinary ring.

In this article we present uncommonly high signal-to-noise mid-resolution near-IR spectra of SS 433. These data enabled us to identify the accretion disc and its outflow. We observed SS 433 every night over an entire orbital cycle with the UIST spectrograph on UKIRT, from 2006 August 17 to August 29, during which time the precession phase varied from 0.40 to 0.47, respectively. We use the convention in which orbital phase (φ_{orb}) zero is when the donor star is eclipsing out, or "blocking from view", the compact object (see Figure 2).

Deconstructing the Br-γ Stationary Line

The stationary Br-γ emission lines show a much more complex profile than the quiescent Hα line studied by Blundell et al. (2008). After trying with different numbers of Gaussian components we came to the realisation that up to six components were needed to account for the complexity of the Br-γ profile shape. Figure 1 (upper panel) shows an example of a fitted Br-γ profile; the six components are coloured light-grey, dark-grey, red and blue.

Figure 1 (lower panel) shows the components of the stationary Br-γ line as a function of time. It is easy to see that the Br-γ complex can be decomposed in to three main constituents: a very broad wind component present at all times in our dataset, and two sets of narrower pairs.

The broad components plotted in Figure 1 show line widths varying from 1300 up to 1500 km/s . The presence of a broad wind component has been reported before from Hα stationary line analysis but with a width reaching only up to 800 km/s (Falomo et al. 1987) and 700 km/s during the quiescent period reported by Blundell et al. (2008). By using the luminosity of this broad Br-γ component as a mass-loss tracer we

(SS 433, continued on page 17)

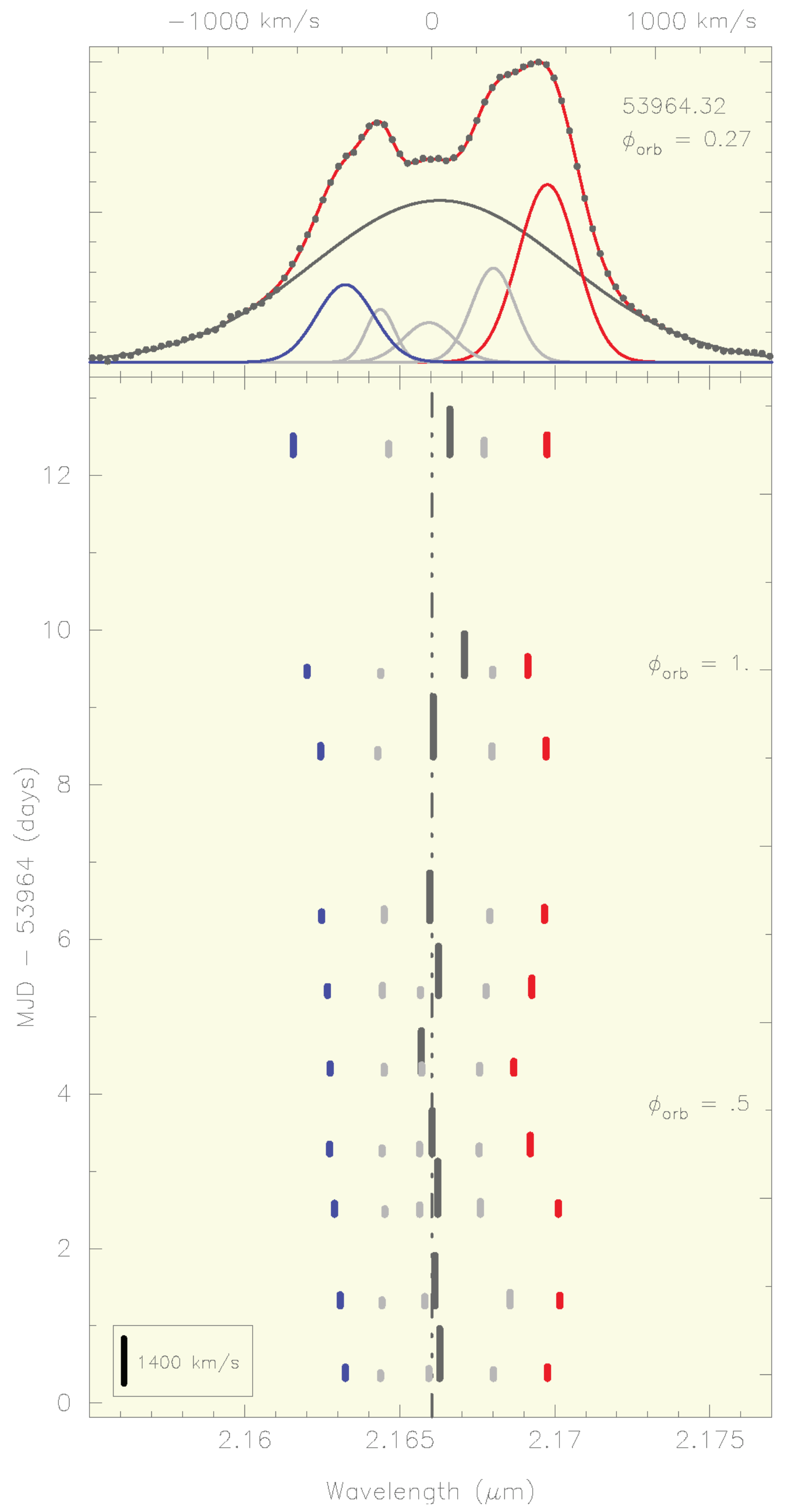

Figure 1. — (upper panel) Example of the Br-γ stationary emission line observed at orbital phase φ_{orb}=0.27. The data (the dots) have been fitted with six gaussian components (plotted in dark-grey [broad wind component], light-grey, red and blue). The red and blue components correspond to the rapidly-rotating accretion disk referred to in the text. The sum of these six components is plotted over the data points in red. The x-axis at the top of this plot gives the velocity scale; it corresponds to heliocentric speed in units of km/s. (lower panel) Tracks of the centroids of the six Gaussian components fitted to spectra observed at different orbital phases (on different dates). The tick mark heights are proportional to the width of each component (see scale in the lower-left corner).

(SS 433, continued from page 16)

have been able to estimate a new upper limit for the rate at which SS 433 is losing mass through its accretion disc wind; our analysis yields a mass-loss rate, $M_{wind}=10^{-4}$ $M_{\odot}$/yr. This, together with the newly (upwardly) determined masses for the components of the SS 433 system, results in an accurate diagnosis of the extent to which SS 433 has "super-Eddington" outflows: its accretion rate is $10^4\times$ higher than the Eddington limit (Perez & Blundell 2009).

The inner set of narrow lines, moving at speeds of ~200 km/s, are fairly steady in wavelength, in excellent agreement with the presence of a circumbinary ring, as reported by Blundell et al. (2008).

The most striking discovery that arises from the Br-γ line modelling is the presence of a pair of widely-separated — hence rapidly rotating — narrow components (Perez & Blundell 2009). An example of these narrow (but widely separated) pairs is depicted in red and blue colours in the upper panel of Figure 1. The speed with which the radiating material spirals in the accretion disc corresponds to half the difference of the speed of those lines, under the assumption that the fitted positions of the lines correspond to the tangent speed. This reveals material that is spiralling in the gravitational potential of the black hole at speeds of about 500 km/s.

Implications for the Geometry of the System

Recently, Blundell et al. (2008) found that the total mass of SS 433 is approximately 40 $M_{\odot}$. We can roughly estimate the size of the system to be about twice the semi-major axis of the orbit "*a*", as given by Kepler's third law: $4\pi^2 a^3 = P_{orb}^{\ 2}\ G\ M_{sys}$, where P_{orb} is the orbital period and M_{sys} is the total mass of the binary. This relation implies a rather large size for the whole system of $2a$~160 $R_{\odot}$. The radius of the companion star should be R~a/2. Thus, the eclipsing of the widely-separated accretion disc lines implies a maximum radius for the companion star R~40 $R_{\odot}$.

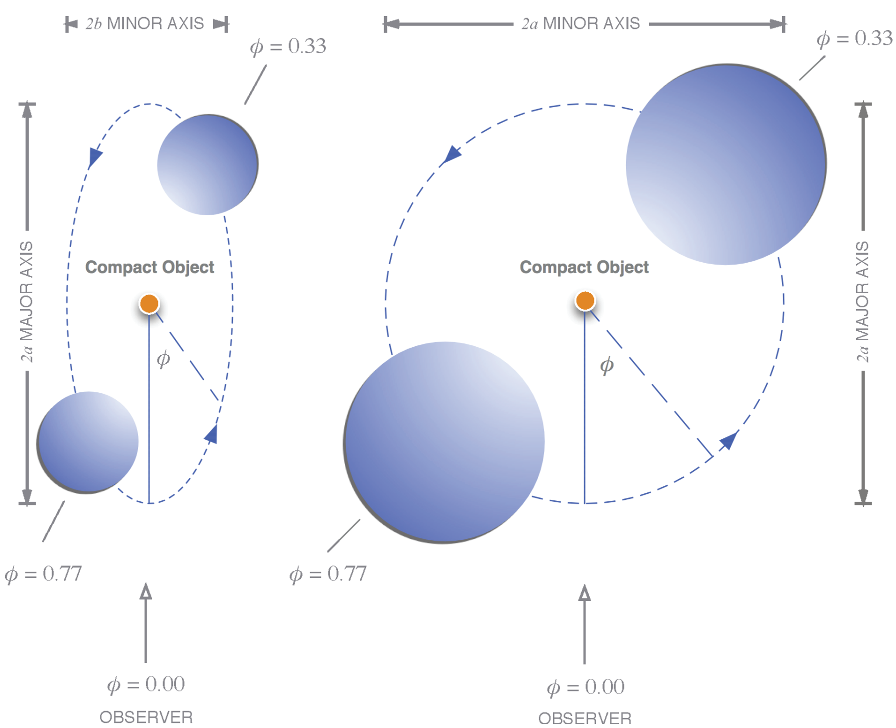

Figure 2. — Diagram that shows the two possible extreme scenarios for the configuration of the SS 433 binary system: (left panel) eccentric orbit, (right panel) circular orbit. One orbital period is the time taken for the companion star (blue circle) to complete an orbit around SS 433's black hole (the compact object), with orbital phase zero being when the companion star is in between us and the black hole. The semi-major axis of the orbit is a~150 $R_{\odot}$.

This size is smaller than, but comparable with, the radius of evolved stars undergoing severe mass-loss such as η Carina (~80 $R_{\odot}$). This large size is reduced only at the expense of accepting an eccentric orbit. The size of the companion star in the eccentric case would be $b=(1-e^2)^{1/2}$ 40 $R_{\odot}$, where *b* is the semi-minor axis of the orbit and *e* is the eccentricity.

Concluding Remarks

Clearly, UKIRT observations have led to a much clearer picture of this remarkable system. Spectroscopic observations taken with UIST have revealed a persistent signature of accretion in SS 433, in the form of two well-defined emission components. The data have confirmed the presence of the circumbinary disc (excretion disc) discovered at optical wavelengths by Blundell et al. (2008). However, they also indicate the presence of a much faster outflow than previously observed. This "fast outflow", where the gas is moving at speeds of approximately 1400 km/s, yields a new upper limit to the rate of mass-loss ($M_{wind}=10^{-4}$ $M_{\odot}$/yr).

Overall, the high signal-to-noise ratio and spectral resolution of our UIST observations have allowed us to deconstruct the many different components associated with the observed Br-γ profile, and thereby unravel the physical processes at work in this binary system.

References

Blundell K.M., Bowler M.G., Schmidtobreick L. 2008, *ApJ*, 678, L47.
Crampton D., Hutchings J.B. 1981, *ApJ*, 251, 604.
Fabian A.C., Rees M.J. 1979, *MNRAS*, 187, 13P.
Fabrika S. 2004, *Astrophysics and Space Physics Reviews*, 12, 1.
Falomo R., Boksenberg A., Tanzi E.G., Tarenghi M., & Treves A. 1987, *MNRAS*, 224, 323.
Ho L.C., Filippenko A.V., Sargent W.L.W., Peng C.Y. 1997, *ApJS*, 112, 391.
McAlary C.W., McLaren R.A. 1980, *ApJ*, 240, 853.
Milgrom M., 1979, *A&A*, 76, L3.
Perez M.S., Blundell K.M., 2009, submitted to *MNRAS*.
Thompson R.I., Rieke G.H., Tokunaga A.T., Lebofsky, M.J. 1979, *ApJ*, 234, L135.

A Near-IR Imaging Survey of High and Intermediate-Mass Young Stellar Outflow Candidates

Watson Varricatt, Chris Davis (*JAC*),
Suzanne Ramsay (*European Southern Observatory-Garching*), Stephen Todd (*Edinburgh*)

From the observational data of nearby star forming regions and through theoretical studies, it is now accepted that low-mass stars form through the accretion of material in molecular clouds (Palla & Stahler 1993). During the process of accretion, they drive collimated outflows. These outflows help us to detect young stars and better understand this accretion process.

When it comes to massive stars, there have been conflicting theories about the mechanism of formation. The large luminosity of the massive stars, which start core nuclear burning before they accumulate all of their mass, is expected to act against further growth through accretion (Stahler et al. 2000).

One school of thought believes that they somehow overcome the radiation pressure and form through accretion. In this case, we expect to see well-defined outflows from the massive YSOs, similar to those driven by their low-mass counterparts (albeit on a larger scale). The other school believes that they form by the merger of lower mass stars (*e.g.*, Bonnell et al. 1998). In this model one would not expect to see well-defined outflows.

Massive stars form in large molecular clouds located mostly in the galactic plane; hence they suffer from large extinction at short wavelengths. Most of the early observations towards massive star forming regions were done using single dish radio and millimeter telescopes, with large beam widths. These gave the impression that outflows from massive young stars are far less collimated than outflows from low-mass young stars. The large degree of clustering seen towards massive star forming regions provided further support to theories of massive star formation through mergers.

The decreasing extinction towards the near-IR enables us to image these objects at greater depth than in the optical, and by using moderately-sized telescopes we attain angular resolutions far better than in the millimetre and radio. Powerful diagnostics of outflows, like the ro-vibrational lines of molecular hydrogen in the near-IR, make this regime highly suitable for searching for outflows from YSOs. To understand the formation of massive stars, we therefore carried out a near-IR imaging survey of massive YSO candidates using UKIRT.

We imaged fifty massive and intermediate-mass YSOs with UFTI. The targets were selected based on their

(YSOs, continued on page 19)

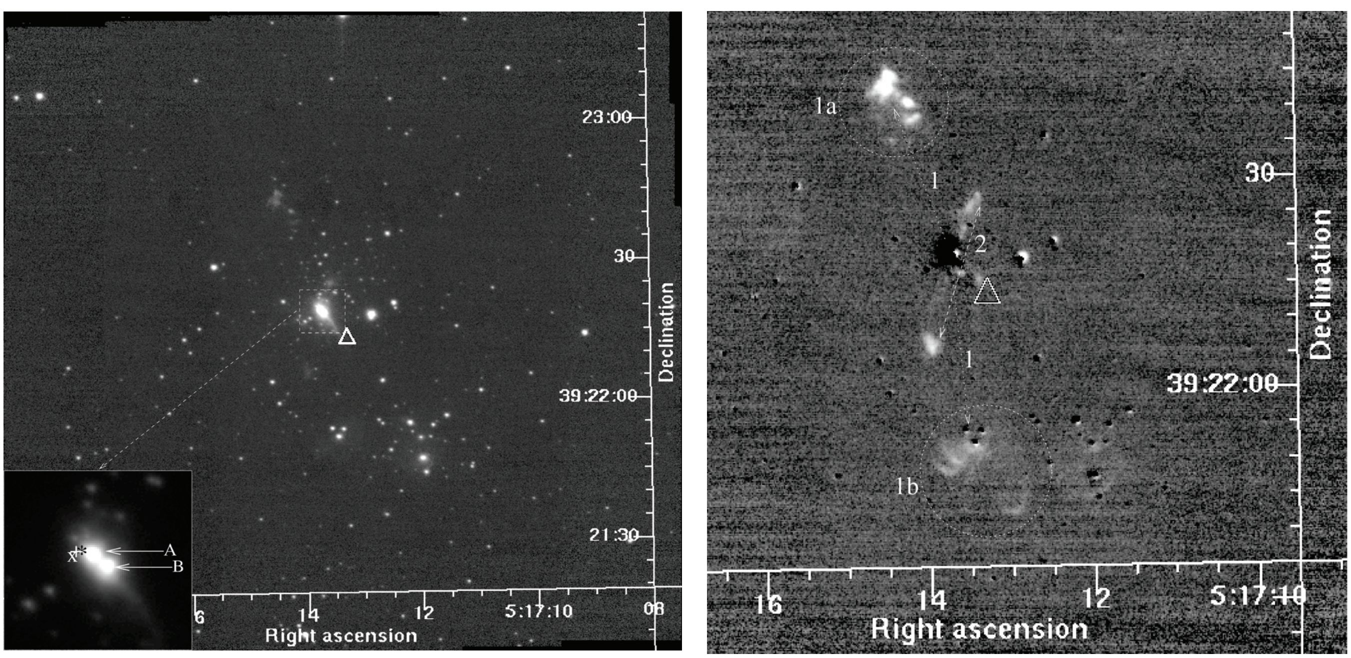

Figure 1. — (left panel) The K-band image of IRAS 05137+3919. A magnified view of the central region is shown inset, with the central binary labelled A and B. The "" shows the position of a 3.4-mm continuum peak in this area; the "×" marks the location of a 3.6-cm radio continuum peak. (right panel) A continuum-subtracted H_2 image of the central region. In this image, H_2 line-emission features associated with at least two outflows are clearly seen. The triangle and "+" mark the positions of IRAS and MSX peaks observed in this region.*

(YSOs, continued from page 18)

mid-IR IRAS colours, the detection of cores in ammonia emission, and the presence of water and methanol masers, which are considered as signposts of massive star formation. Many of these targets were also known to exhibit CO outflows (Molinari et al. 1996, Sridharan et al. 2002). The observations were performed in broad-band *K* and in narrow-band filters centred at the wavelengths of the H_2 *v*=1–0 S(1) and H I Br-γ lines. The H_2 images were used to detect outflows through shocked emission from the region of interaction of the jet with the ambient medium; the *K*-band images were used to continuum-subtract the narrow-band images and to look for embedded objects.

Our H_2 and *K*-band imaging revealed several new outflows and possible young clusters. 76% of the objects surveyed by us display H_2 emission; 50% show aligned knots in H_2 implying the presence of collimated outflows. Moreover, these numbers should be treated as lower limits, since extinction may be hampering the detection of many outflows. Most of the aligned H_2 knots are most certainly due to shocked emission from jets (*e.g.*, Davis et al. 2004, Todd & Ramsay Howat 2006, Caratti O. Garatti et al. 2008). Our data show that, similar to low-mass stars, the outflows in these massive star forming regions are mostly jet-driven (rather than wind-driven). Also, in most regions there is good agreement between the centroids and directions of the outflows deduced from the aligned H_2 knots and those from published CO maps.

Figure 1 shows H_2 and *K*-band images of one of the 50 regions observed, IRAS 05137+3919. The H_2 jets labelled 1 and 2 are probably driven by a pair of objects, labelled A and B in our *K*-band image (inset).

The driving sources for many of the outflows were identified in our *K*-band data with good positional accuracy. The images therefore enable further high angular resolution studies. Figure 2 shows the 2MASS colours of most of these stars, plotted on a "near-IR" colour-colour diagram. A major fraction of these objects are located to the right, in the region known to be occupied by reddened YSOs with excess infrared emission. Many of these are therefore candidate outflow-driving sources.

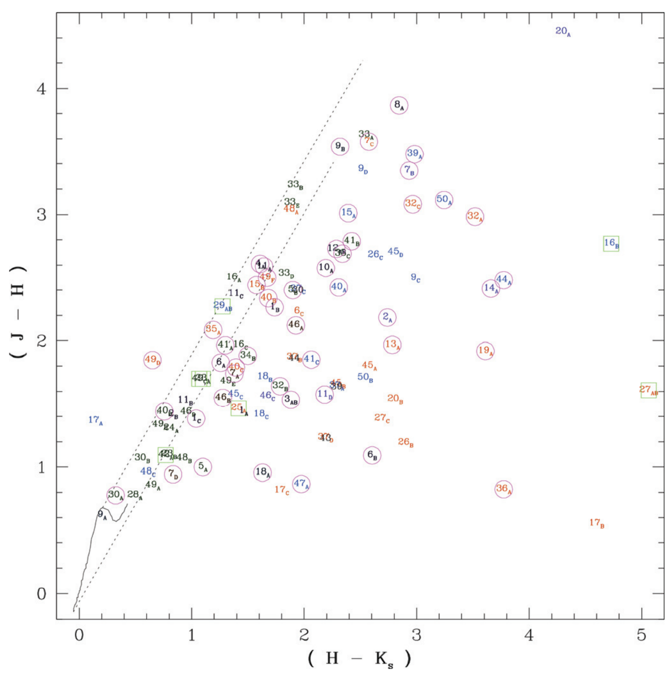

Figure 2. — A near-IR colour-colour diagram produced using 2MASS J,H,K_s magnitudes for near-IR sources in each of the 50 regions observed. The continuous line in the lower-left denotes the location of main sequence stars in this diagramme, while the two dashed lines show the reddening vectors up to an extinction A_v=30. The sources which we identify as the IR counterparts of the YSOs driving the outflows are circled. Sources which are detected by 2MASS in all three bands are labelled in black; those which are detected in only two bands are labelled in blue; those detected in only one band are marked in red. Squares identify the near-IR counterparts of confirmed UCHII regions.

In Figure 2 we also show the locations of the near-IR counterparts of confirmed Ultra Compact H II regions (UCHIIs). UCHIIs, when detected in all three bands, have much less excess (are situated more to the left) when compared to the younger outflow sources. This tells us that, by the time an object has reached the UCHII stage, it has completed a major part of its outflow phase. A large fraction of our objects are thus in the *pre-UCHII* phase; most of these are located in the region of the IRAS "mid-IR" colour-colour diagram occupied by the UCHIIs, defined by Wood & Churchwell. (1989). Therefore, objects identified with the Wood & Churchwell colour criteria mostly represent luminous YSOs, which are UCHIIs and pre-UCHIIs located in clusters.

Our observations also demonstrate a high degree of binarity or multiplicity in each region, although this result requires further verification through other methods. Poor collimation ratios derived from CO maps are, in several cases, due to multiple outflows which are unresolved at the large beam widths of the millimetre and radio observations.

From our extensive dataset and analysis, we infer that objects up to late O form mainly through accretion. However, our sample does not cover the extremely massive stars. These rare objects will require further investigation.

References

Bonnell I.A., Bate M.R., Zinnecker H., 1998, *MNRAS*, 298, 93.

Caratti O Garatti A., Froebrich D., Eisloeffel J., Giannini T., Nisini B., 2008, *A&A*, 485, 137.

Davis C.J., Varricatt W.P., Todd S.P., Ramsay Howat S.K., 2004, *A&A*, 425, 981.

Molinari S., Brand J., Cesaroni R., Palla F., 1996, *A&A*, 308, 573.

Palla F., Stahler S.W., 1993, *ApJ*, 418, 414.

Sridharan T.K., Beuther H., Schilke P., Menten K.M., Wyrowski F., 2002, *ApJ*, 566, 931.

Stahler S.W, Palla F., Ho P.T.P., 2000, in *Protostars and Planets IV*, ed. V. Mannings, A.P. Boss, S.S. Russell, Univ. Arizona Press, Tucson, p.327.

Todd S.P., Ramsay Howat S.K., 2006, *MNRAS*, 367, 238.

Wood D.O.S., Churchwell E., 1989, *ApJ*, 340, 265.

25 Years of Service Observing at UKIRT (and Counting...)

Chris Davis (*UKIRT Senior Support Scientist*)

Versatility and opportunity have always been key pieces of the observing puzzle at UKIRT. This is particularly true with the Service observing programme, which has been in operation since the early 1980s.

UKIRT was officially opened in October, 1979. Two of UKIRT's first instruments were UKT1 and UKT2, each a single-channel photometer/scanner working with a focal-plane chopper. The suite of detectors rapidly expanded (see Table 1 and Figure 1), and it was not long before a service observing programme was proposed. Andy Longmore recalls suggesting in 1983 (or there abouts) a means by which U.K. astronomers could obtain quick follow-up observations to discoveries made with the soon-to-be-launched IRAS satellite. Such fast-track data collection might give UK astronomers an edge in the rapidly-advancing field of infrared astronomy. With email now linking astronomers across the globe, peer review of proposals without the panel ever having to meet was now a possibility. Tim Hawarden, based at the Royal Observatory, Edinburgh at the time (though part of the UKIRT Division), suggested extending "IRASserv" to include any fast-turn-around observations. A fully fledged service programme would also allow astronomers to try out ideas before putting in full PATT proposals, and would facilitate synoptic studies that required relatively brief observations of slowly-varying objects spread over months or even years. The idea for UKIRTserv was put to the UKIRT Users Committee, and soon after, the Service observing programme was born.

By 1984 the programme was in full swing, and had already been awarded "long-term" status by the UKIRT Panel for the Allocation of Telescope Time (PATT). One of the first service projects undertaken was photometry of a supernova in NGC 991. The PI of the project, J. Graham (Imperial College, London), later reported in an *IAU Circular* that "the object has been designated as both Type I and Type II. The blue *H–K* colour [from the UKIRT observations] is atypical of Type II but similar to the colours of Type I supernovae". The supernova was later defined as a peculiar (under-luminous) Type I object.

Right from the start, a wide range of projects were attempted in service mode: from spectroscopic monitoring of Nova Vul between 1 and 4 μm to *J*-band spectroscopy of the active galaxy NGC 5506 (Figure 2); from some of the first maps and spectroscopy of molecular hydrogen line emission in outflows from young stars (Figure 3), to monitoring of "BL Lac type and Quasar-like" sources; from imaging of edge-on spiral galaxies and galaxies with cooling flows to spectroscopy of silicate features in galactic IRAS sources. At the time, these were often ground-breaking and very exciting observations!

Tom Geballe, staff astronomer at UKIRT from 1981 to 1990 and Head of Operations from 1990 until late 1998, remembers one of the first service nights with CGS4. On June 29, 1991, Tom was the observer. He recalls that "the service night occurred after two array detectors had been damaged and we were down to the engineering detector — which turned out to be more stable and in some ways better than the 'science grade' arrays; the engineering device lasted until it was replaced by the (current) 256×256 array in 1995. CGS4 had been put on the telescope in the spring of 1991, although not a lot of science had been done with it up to that

(Service Observing, continued on page 21)

Figure 1. — A youthful Jay Tsutsumi tops up the liquid nitrogen in UKT6 at the Cassegrain focus of UKIRT (c. 1982). UKT5 can be seen to its left. (Image courtesy Royal Observatory Edinburgh.)

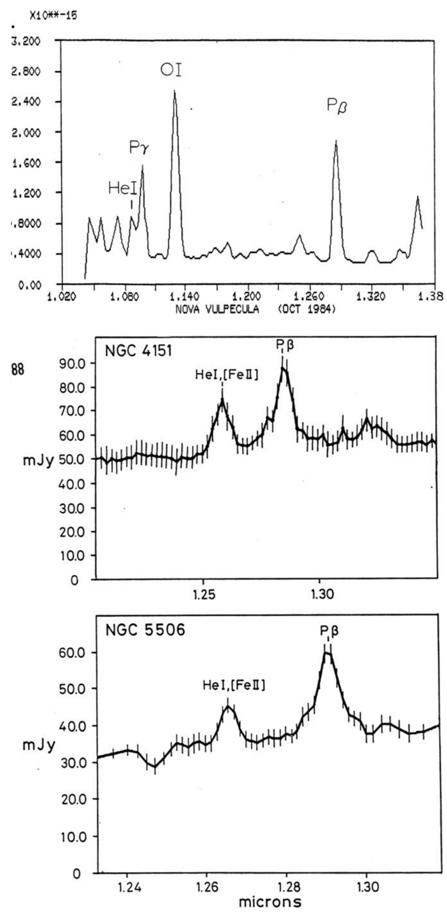

Figure 2. — (upper panel) A CGS2 spectrum of Nova Vul 1984 No. 1 (=PW Vul) taken in October 1984. This was one of a series of spectra covering 1–4 μm, taken at 2 month intervals following the Nova event. At the time, suggestions were sought for the non-H and non-He transitions seen in the spectra. In 1984 a second nova in Vulpecula (Nova Vul 1984 No. 2!) was also observed in UKIRT service time. (lower panels) A CGS2 spectrum of the active galaxy NGC 5506. Near-IR data were needed to probe the dust-obscured nucleus of this galaxy. These service data, acquired in 1988 as a pilot study for Martin Ward et al., revealed for the first time both narrow and broad components to the Pa-β line, demonstrating the true nature of this Seyfert 1 nucleus (the Seyfert 1 galaxy NGC 4151 was observed for comparison).

Table 1.
Three Decades of Common-User
Cassegrain Instrumentation at UKIRT

Instrument	Description	Commis-sioned
UKT1	Single channel photometer	1979
UKT2	Single channel photometer	1979
UKT3*	Polarimeter module	~1980
UKT4*	TV camera guider cross-head	~1980
UKT5	Single channel InSb photometer with 1.3–2.6 µm CVF	1981
UKT6	Single channel InSb photometer with 2.4–4.8 µm CVF	1981
UKT7 (Little Bertha)	Single channel bolometer with LMNQ + NB filters	1983
UKT8 (Big Bertha)	Single channel bolometer with 3–13 µm CVF	1984
UKT9	Single channel InSb photometer with 1.3–2.6 µm CVF	1984
UKT10 (2-Banger)	2-channel near-IR InSb photometer	1983
UKT14	Single channel sub-mm bolometer	1986
UKT16 (8-Banger)	8-channel mid-IR bolometer	1984
IRASFU	16-channel mid-IR SiAs photometer	1984
CGS1	Single channel 1–5 µm grating spectrometer	1982
CGS2	7-channel 1–5 µm grating spectrometer	1983
CGS3	32-pixel 8–14 µm grating spectrometer	1990
CGS4	1–5 µm grating spectrometer with 58×62 pixel array	1991
IRCAM	1–5 µm imager with 58×62 pixel array ("UKIRT's first near-IR imaging system")	1986
IRCAM3	1–5 µm imager with 256×256 pixel array	1994
UFTI	1–2.5 µm imager with 1024×1024 pixel array	1998
UIST	1–5 µm imager-spectrometer with 1024×1024 pixel array and Integral Field Unit	2002
Michelle	10–20 µm imager-spectrometer	2001
IRPOL	1–5 µm polarimetry unit	~1984
IRPOL2	1–5 µm polarimetry unit	1995

* Perry Williams recalls that "UKT3 was known as the 'toilet seat' polarimeter, built by Peter Brand and Chris Impey, which rotated a polaroid filter above the focal plane chopper and led to a lot of publications on polarimetry of BL Lac objects. The polaroid could be raised, hence the name. UKT4 was the cross-head for the TV guider. These [UKT] numbers were allocated in the instrument control program presumably so that they could be used in rows of coefficients in data tables, which is why the next photometers were called UKT5 and UKT6."

(Service Observing, continued from page 20)

point, because of various problems. But that service night really showed what CGS4 could do. Among a number of high quality measurements, we got a *K*-band spectrum of Triton that clearly showed absorption bands of solid CO_2, solid N_2, and solid CO, in addition to the solid CH_4 already known. The spectrum was vastly superior to any of Triton obtained previously. I remember Dale Cruikshank, the PI of the Service proposal writing to me that he was 'blown away' by the spectrum, and I used that quote when I reported to the UKIRT Board later that year. Another spectacular spectrum obtained that night was one of Cygnus X-3, revealing for the first time that the companion to the neutron star or black hole was a Wolf-Rayat star. The latter resulted in a publication in *Nature*."

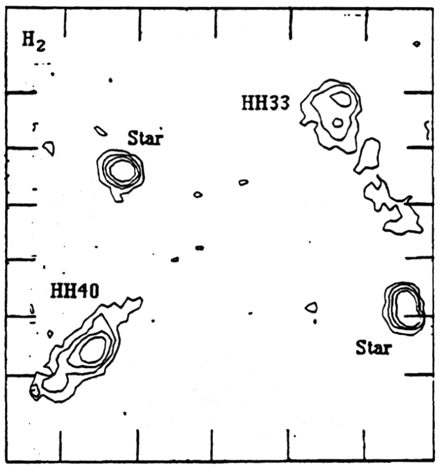

Figure 3. — An IRCAM image of Herbig-Haro objects 33 and 40, obtained in 1988 for Zealey, Williams, Sandell et al.

Even during the early days of Service observing, multiple instruments were available at UKIRT (see Table 1 and Figure 1). Although switching between Cassegrain instruments was less straight-forward than it is today, it was not impossible and multiple projects could be attempted during a single night. In some respects the Service programme represented UKIRT's first dalliance with flexible scheduling!

Service observations have often been used to complement data taken with multiple facilities. In their 2003 paper, for example, Sylvain Chaty (Paris) and collaborators obtained UFTI, IRCAM3 and CGS4 observations of the soft X-ray transient XTE 1118+480 (a class of low-mass X-ray binary). Taken throughout 2000, they complemented these data with HST, RXTE and Extreme Ultraviolet Explorer observations as well as archival VLA, JCMT, Chandra and SAX data, and constructed a near-complete spectral energy distribution (SED) that stretched from the X-ray to the radio. With data taken over seven epochs, they were able to analyse the evolution of the SED during the outburst, assessing the contributions from the companion star, the accretion disc, and the outflow.

(Service Observing, continued on page 22)

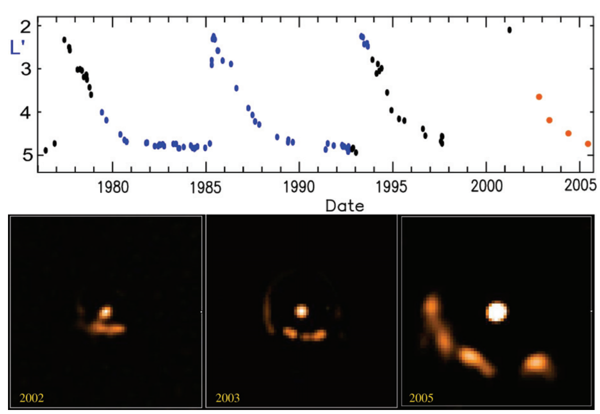

Figure 4. — (upper panel) An L'-band light curve of the Wolf-Rayet binary WR 140 obtained at UKIRT and elsewhere over a period of 25 years (UKIRT data coloured blue and orange). These data led to the discovery that the periodic variations in the brightness of WR140 (and similar objects) are due to dust formation caused by the interaction of stellar winds from two massive stars (the Wolf-Rayet star and its O-star companion). The winds collide when the component stars come close during periastron passage. (lower panels) The three 4 µm images, each only 4×4" in size, show the latest data collected using UKIRT and UIST. The excellent image quality and sensitivity enabled the imaging of the dust shell formed during the 2001 periastron passage; its expansion and cooling are evident in the 2003 and 2005 images.

View from the Top

Thor Wold (*UKIRT Telescope System Specialist*)

As you have seen from the articles in this edition, we had quite a successful Cassegrain observing block this last winter. This will be the last for a year — maybe forever. Since the end of the block the weather has deteriorated considerably — diametrically opposite to early 2006 when we had the Biblical Flood that entirely wiped out that whole Cassegrain allocation. So, this one was good retribution (especially if it does turn out to be the last Cass block).

And so, since then we have had some pretty nasty weather and, since the return to WFCAM, have seen hardly any photons. Lots of heavy high clouds, as well as the usual fog/ice/snow. At my home in upper Hilo I have clocked 80" of rain between the start of the year and March 30 — so 80" in just 88 days. We have even gotten some much-needed moisture in the uplands, and the spring flowers are starting to bloom around Hale Pohaku.

Speaking of Hale Pohaku, at the end of January Mauna Kea Support Services announced they were closing down Building D due to a budgetary shortfall. It seems the break-even point is around 27 residents per day and they were under this quite often. I think it has picked up a bit since the Holidays, but it is still on the edge or under this limit on weekends.

(View from the Top, continued on page 23)

(Service Observing, continued from page 21)

Service observing has always been useful for long-term monitoring projects. A wonderful example of this was reported in the September 1999 issue of this *Newsletter*. Peredur Williams (Edinburgh) and collaborators had at that time spent over 20 years monitoring episodic dust formation by a small group of WC-type Wolf-Rayet stars in colliding-wind binary systems. The dust emission peaked in the *L*-band, so UKIRT, with its service programme and suite of InSb photometers and cameras, provided the best opportunity for undertaking this project, which continued well into the 21st century (see Figure 4)!

Although traditionally polarimetry has not been offered in service mode, in recent years imaging- and spectro-polarimetry have become fairly run-of-the-mill, especially with UFTI and UIST. This is largely due to improvements in software, both in terms of target acquisition and data reduction. The commissioning of a reliable system (IRPOL2) and the subsequent characterisation of that system in the late 1990s by Jim Hough and Antonio Chrysostomou (Hertfordshire) also played a significant role. In 2006, buoyed by the success of a number of PATT projects that had utilised IRPOL2, we decided to put out a call specifically for linear and circular polarimetry projects. The call proved popular, and in subsequent service nights a number of polarimetry projects were attempted. These included spectro-polarimetry of CO bandhead emission in protostellar accretion disks (Dent/Edinburgh) and imaging-polarimetry of nebulae associated with Herbig-Haro energy sources (Froebrich/Kent). Polarimetry remained as an option for all future service rounds.

Service observing continued as an integral part of the Cassegrain programme at UKIRT, right up until the switch to wide field mode in January of this year. Indeed, a number of service projects were finished off on the very last night of the Cassegrain block. These projects included: short-*L* UIST spectroscopy of a luminous infrared galaxy, using PAH bands to map star formation and the continuum and 3.4 μm absorption to trace the AGN (Zijlstra/Manchester); *L*-band spectro-polarimetry of the post-AGB star Frosty Leo, to search for aligned, non-spherical dust grains (Murakawa/Bonn); and *IJHKL* spectroscopy of pulsating carbon stars, to constrain models of their atmospheres (Hron/Vienna).

But the story does not end here; the Service programme lives on with WFCAM — still the world's most powerful infrared survey camera! Service nights have been scheduled throughout 09A and we plan to continue the programme for the foreseeable future. Currently active programmes include: the mapping of jets and outflows over vast regions in Orion B, observations which will complement the JCMT Legacy Survey of the Gould Belt (Buckle/Cambridge and Davis/JAC); photometry of a metal-rich open cluster at high galactic latitude, to examine the mass function across and well below the stellar/substellar boundary (Jameson/Leicester); and imaging of a double galaxy cluster, so that the ages and metallicities of the bulge and disk components can be measured separately, and the effect of the cluster environment in quenching the disks can be examined (Smith/Durham).

Although the suite of Cassegrain instruments will certainly be missed, opportunities remain for those seeking a few hours of data to finish off an existing project or as a pilot study for a new endeavour. With WFCAM, the future for the UKIRT service observing programme remains bright.

Further details of the UKIRT Service Observing programme are available from the link on the sidebar of the UKIRT homepage, or at: `http://www.jach.hawaii.edu/UKIRT/service/` .

Acknowledgments

A huge thanks to Tom Geballe, Perry Williams and Andy Longmore for their help in putting this article together; without their long memories we would certainly have been lost. Thanks also to the many (unpaid) Service referees who, over the years, have made sure we haven't been wasting valuable telescope time on wild goose chases. There are too many to name, but its certain that the Service observing programme would not have been possible without them.

(View from the Top, continued from page 22)

However, they wisely took this down-time on Building D to do some much needed renovations. They have now re-opened D while they close Building C to do the same. If you are a regular reader of this space, you will know that there is apparently a long-term project, begun in the summer of 2004, to replace the exterior siding of Building B. In the last *Newsletter* I reported that work was again commencing on this project. However, this turned out not to be the case and the scaffolding still sits, unused, on the mountain side of the building (nice views from that side!). This project will celebrate (or not!) its 5th birthday this summer.

Meantime, they have also instituted some money-saving measures. You will often find the pool-table and dining areas of the Commons Building unlit. The selection of canned drinks has gotten much smaller, and there are pleas everywhere to conserve water and electricity. The utensils at HP tend to disappear and they have been replacing them recently with some inexpensive stuff from China that seem to have the consistency of tin. I find myself having to straighten the tines on forks and re-shape the handles on spoons quite often. I suppose utensils that fall victim to the garbage disposal will no longer be recycled back into use. Next time you visit us, all together now... format your forks!

The new section of Saddle Road was officially dedicated back in early December, well after it was put to good use. The Federal Highway Administration (FHA) was so pleased with the quality of the pavement that they awarded a 5% cash bonus to the contractor; they were so pleased with the quality of the asphalt — which was mixed alongside the project to reduce the number of trucks going up and down the road — that they awarded an additional 4%! From my view, it is certainly worth it. It must be the best stretch of highway in the whole state.

The same contractor got the job of finishing the stretch that runs behind the Pohakuloa Training Area, from the 35 to 42 mile-posts; the grading had already been done some time ago and they only have to create the two ends and pave the seven miles, which will then mean a continuous 21 miles of new road.

Bids will be let in summer for the next project, which is supposedly the stretch from mile-post 6 at the top of the new Puainako Street extension on up to the 19-mile mark where the new road now starts. In order to maintain FHA funding, contractors must initiate things by August, so be prepared if you have to drive up to Hale Pohaku as there may again be heavy construction happening. The road will follow the basic footprint of the existing road. They have just started drilling bore holes along the route to test the underlying lava. No completion date has been published yet. This stretch is hoped to come in at around $80 million (the saddle thus far has cost $124 million).

UKIRT celebrates its 30th birthday in October! A nice article covering 29 years of Cassegrain Service observing appears in this edition. I have been working here since summer 1985, so have been privy to many of the instruments mentioned, and of course went through the commissioning process on those that appeared after that date.

One of the most amazing things about Cass observing at UKIRT has always been the ease of use and speed with which we could swap instruments; we have a dichroic mirror that can be rotated to one of four ports under the primary mirror, where four instruments (or more, actually) can be mounted. Thus, it takes only a few minutes to position the dichroic facing an instrument. Additionally, the software, which has been developed over many years, allows the observer to very easily switch the software controls to the next instrument. This all happens while the mirror is in motion so that all is ready once the mirror gets into position. Consequently, if weather conditions changed, *e.g.*, if thin clouds rolled in, we could switch from photometry to spectroscopy without losing any time to speak of.

A good example of this was the Comet Shoemaker-Levy 9 collision with Jupiter on July 20, 1994. By then of course the comet had split into many fragments, measuring between a few hundred meters to a couple of kilometers in size. As many readers will remember, on this particular night the biggest chunk was set to collide with Jupiter. However, the impacts took place on the side of the planet facing away from us, so we had to wait for Jupiter to rotate the impact sites into view.

I remember figuring maybe I would see something on the TV guider (these were the days before guiding on a CCD camera). The TV screen was about 8×8 inches in size, and Jupiter filled about a quarter of the screen. Like me, Tom Geballe, who was at the telescope for the collision, thought that maybe the event was going to be weaker than it was... when the horizon rolled over into our field of view, my jaw dropped! There was a huge "hole" in the planet — bigger than the red spot! Our first spectra were enormously saturated, so we stopped, Tom changed the exposure time, and we were back in business in a matter of moments.

While everyone else seemed to be busy taking pretty pictures, we had CGS4 running and so were seeing the physics of the event. The phone started ringing immediately because scientists everywhere wanted to know if we were detecting water vapor!

Over the years, the systems on UKIRT have certainly evolved, and continue to evolve, to be facile; all of this gained from hands-on observational experience over time. Ask anyone who has used this facility and they will tell you that our efficiency is tops. Minimal time taken for set-up, and a data reduction pipeline second to none. It will certainly be very sad if we don't in future years return to Cassegrain observing at UKIRT.

Aloha!

Future Instrumentation Updates *International Year of Astronomy 2009 Events*

www.jach.hawaii.edu/UKIRT

jk